

Review

Preparation Techniques of TiO₂ Nanofluids and Challenges: A Review

Hafiz Muhammad Ali *, Hamza Babar , Tayyab Raza Shah, Muhammad Usman Sajid ,
Muhammad Arslan Qasim and Samina Javed

Mechanical Engineering Department, University of Engineering and Technology, Taxila 47050, Pakistan; engr.hamza080@gmail.com (H.B.); tayyabrazahashmi@gmail.com (T.R.S.); usajid976@gmail.com (M.U.S.); arslanqasim993@gmail.com (M.A.Q.); saminajaved073@gmail.com (S.J.)

* Correspondence: h.m.ali@uettaxila.edu.pk

Received: 10 February 2018; Accepted: 26 March 2018; Published: 8 April 2018



Abstract: Titanium dioxide (TiO₂) has been used extensively because of its unique thermal and electric properties. Different techniques have been used for the preparation of TiO₂ nanofluids which include single-step and two-step methods. In the natural world, TiO₂ exists in three different crystalline forms as anatase, brookite, and rutile. Nanoparticles are not used directly in many heat transfer applications, and this provides a major challenge to researchers to advance towards stable nanofluid preparation methods. The primary step involved in the preparation of nanofluid is the production of nano-sized solid particles by using a suitable technique, and then these particles are dispersed into base fluids like oil, water, paraffin oil or ethylene glycol. However, nanofluid can also be prepared directly by using a liquid chemical method or vapor deposition technique (VDT). Nanofluids are mostly used in heat transfer applications and the size and cost of the heat transfer device depend upon the working fluid properties, thus, in the past decade scientists have made great efforts to formulate stable and cost-effective nanofluids with enhanced thermophysical properties. This review focuses on the different synthesis techniques and important physical properties (thermal conductivity and viscosity) that need to be considered very carefully during the preparation of TiO₂ nanofluids for desired applications.

Keywords: titanium dioxide; nanofluids; anatase; brookite; rutile; synthesis techniques; thermophysical properties; heat exchangers

1. Introduction

Scientists and researchers introduced a new class of fluids known as nanofluids, prepared by dispersing nanometer-sized materials in the form of nanotubes, nanofibers, nanoparticles, nanowires, droplets and nanosheets into the base fluid, that have comparatively low values of thermophysical properties like thermal conductivity, thermal diffusivity, viscosity, etc. In the past, many additives have been used in base fluids, but nanofluids were found most suitable to ameliorate heat transfer characteristics. When we look back at the history of nanofluids, the technique of improving the thermal conductivity of single-phase fluids with the addition of solid particles was first reported by Maxwell [1] in 1873. At that time the technique failed to gain the attention of scholars and investigators due to various problems, such as sedimentation, clogging and erosion during the flow. Later, in 1993, Masuda et al. [2] carried out the work of Maxwell and observed the enhancement of thermal conductivity with the addition of micro-sized solid particles into the base fluid. They succeeded in preparing a fluid with enhanced thermal conductivity, but the problem of sedimentation of solid particles into the base fluid reduced its performance. In 1995, Choi [3] moved one step forward and introduced the nanofluids by dispersing the nanosized solid particles into the base fluid. The prepared fluid

showed better performance with enhanced thermophysical properties without creating considerable stability problems. Fine particles in the range of millimeters and micrometers failed to exhibit better heat transfer performance because of obstacles such as particle sedimentation, excessive pressure drop, low thermal conductivity, corrosion of components and particle clogging, etc. This problem can be mitigated by suspending the nano-sized particle in the range of 100 nm in the suitable volume fraction of conventional base fluid. Ultrafast heat transfer, adequate durability, negligible agglomeration, stable dispersion, reduction in pumping power and better lubrication are the important features of nanofluids. All the nanoparticles that have a high thermal conductivity include metallic (Ag, Cu, Al, Fe, Au, etc.) and non-metallic (TiO₂, CuO, Al₂O₃, SiC, Carbon nanotubes, Fe₃O₄ etc.) particles can be used as an additive for the preparation of nanofluid in the presence of base fluid. Among all these nanoparticles, TiO₂ nanoparticles are used most commonly due to the stability of its chemical structure, electrical, optical, biocompatibility, and physical properties. We can easily understand the prodigious heat transfer feature from the Newton's law of cooling.

$$Q = h \times A \times \Delta t \quad (1)$$

Nanofluids can be helpful for enhancing the rate of heat transfer (Q) by increasing the convective heat transfer coefficient (h) for a constant value of heat transfer area (A) and temperature difference (Δt) due to the enhanced thermal conductivity. When the nanosized solid particles are dispersed into the base fluid each particle absorbs and desorbs an electron at the interface with the base fluid and gets electrically charged [4]. In the case of stable nanofluids, the Vander Waals repulsive forces become larger compared to the attractive forces between the particles and the Brownian motion is enhanced. Brownian motion plays a significant role in increasing the thermal conductivity by enhancing micro-convection due to the transfer of heat between solid particles during their collision [5–7].

A lot of research has been conducted on the preparation methods of TiO₂ nanofluids because of its wide industrial and commercial applications in almost every sphere of life particularly in electronic devices [8,9], heat sinks [10–16], solar energy [17–21], the automotive industry [22–27], heat exchangers [28–33] and nucleate pool boiling [34–37].

2. Preparation Methods

The preparation of nanofluid is not just a simple process of mixing the nanoparticles into the base fluid. To get nanofluids with homogeneously dispersed nanoparticles, stabilization and proper mixing are required under certain environmental conditions. There are many methods used for the preparation of nanofluids, which can be classified into two primary classes according to the number of steps involved during their preparation.

Figure 1 shows the classification of the different methods involved in the preparation of TiO₂ nanofluids and Table A1 in Appendix A shows a summary of the related studies using these methods and techniques.

2.1. Single Step Method

Single step methods involve the preparation and suspension of nanoparticles into the base fluid, but both processes are carried out at the same time as shown in Figure 2. Storage, drying, transportation, and dispersion are avoided in the single step method, so that the dispersion of nanoparticles in the base fluid is improved while agglomeration is minimized.

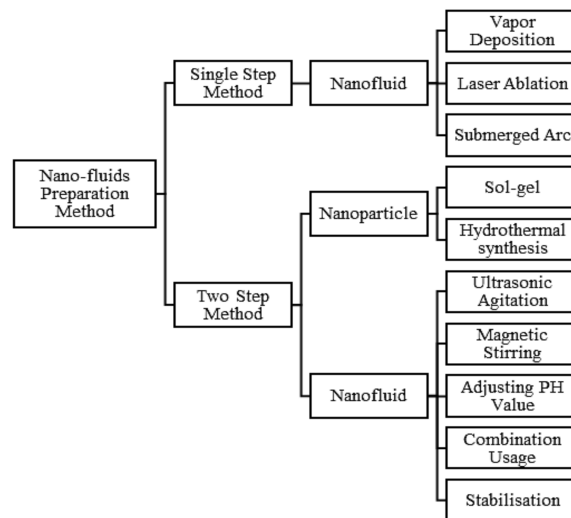


Figure 1. Classification of preparation methods.

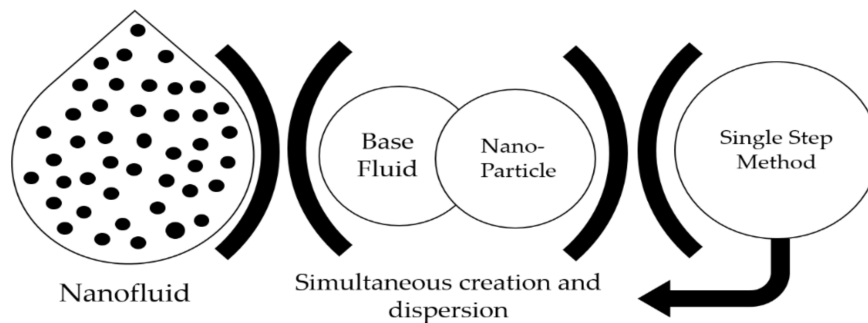


Figure 2. Single step method.

2.1.1. Vapor Deposition

Choi and Eastman [38] developed the vapor deposition (VDP) method in 2001, and this is the most used single step method in recent decades. As shown in Figure 3, a thin layer of base fluid is formed on the vessel wall under the action of the centrifugal force of the rotating disc. The material is heated and evaporated in a container filled with an inert gas at low pressure. Nanofluid is obtained when the vapors of the raw material are condensed via interaction with a thin film of swirling water and settle in the base fluid.

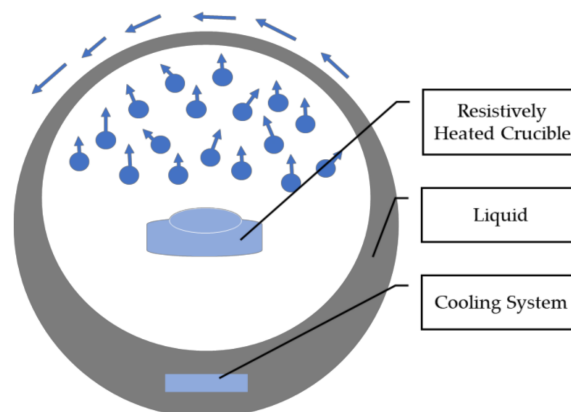


Figure 3. Schematic diagram of vapor deposition method.

The pulsed wire evaporation (PWE) method is an improved single-step vapor deposition method used to prepare nanoparticles with higher thermal characteristics. Experimental apparatus is comprised of four central components: an evaporation/condensation chamber, a high voltage dc power supply, a capacitor bank and a high voltage gap switch. A thin wire of titanium that is induced in the reaction chamber is evaporated into the plasma within a few microseconds when the pulsed high voltage drives through the wire. The inner wall of the reaction chamber is covered with base fluid and a nozzle spray system in which the exploited wire nanoparticles are condensed by direct contact with the base fluid without any surface contamination. Lee et al. [39] prepared ethylene glycol based TiO₂ nanofluid by using the pulsed wire evaporation method. Pure titanium nanowire with a diameter and length of 0.5 mm and 100 mm, respectively, was used during experimentation. Ethylene-glycol, comprising nanoparticles of size less than 100 nm were successfully prepared with enhanced thermal conductivity. Results showed that the thermal conductivity of the prepared nanofluids was enhanced by increasing the volume concentration of nanoparticles but no particular effect with temperature variation was noticed.

The vapor deposition method is mostly used in the preparation of nanofluids but is also less commonly employed in the case of TiO₂ nanofluids because it required a higher temperature to evaporate the material placed in the evaporation chamber. The VDP technique was further extended by introducing the laser ablation method and sub-merged arc method that removes the limitation of evaporating the materials, which requires higher temperature during the preparation process.

2.1.2. Laser Ablation Method

This is a technique used to disperse the nanoparticles from the surface of the material submerged in the base fluid by irradiating it with a highly focused laser beam. The depth of the submerged material depends upon its optical properties, the amount to be removed and the laser intensity and wavelength. Huang and Zhang [40] prepared TiO₂ nanofluid under a nitrogen-free atmosphere by submerging the anatase type TiO₂ into the flowing fluid as shown in Figure 4.

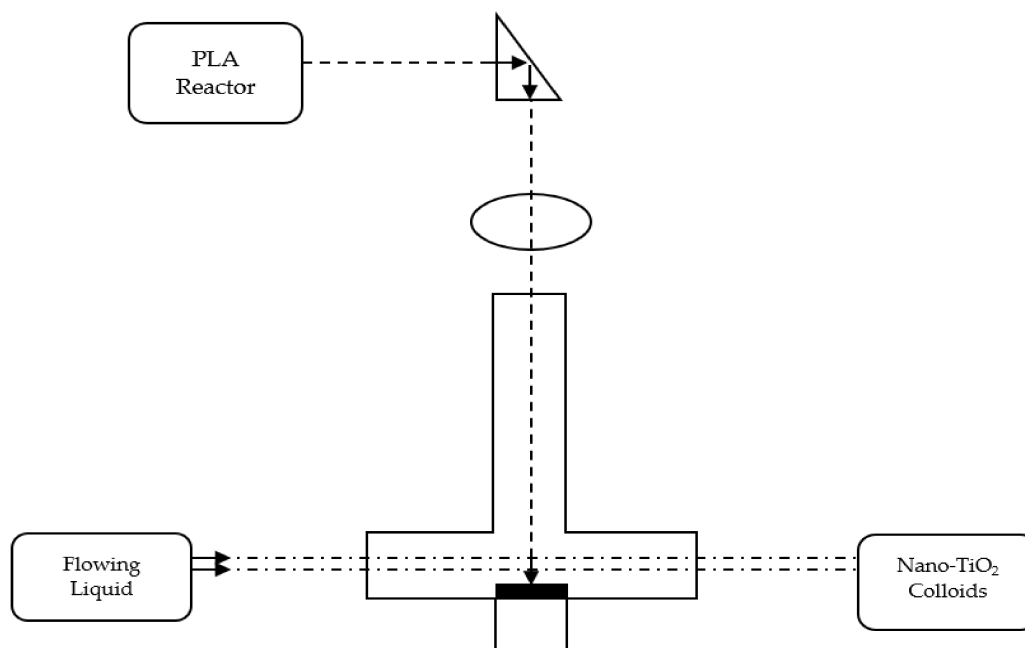


Figure 4. Pulsed laser ablation (PLA) model schematic diagram [40].

They used three different base fluids (anhydrous ethanol, cyclohexane, water) during the experimental study and found that anhydrous-ethanol was the best flowing fluid under conditions of low flow rates (0.017–0.15 mL/s). Supreme pulsed laser output power (100–250 mJ/pulse) and with appropriate aging time, nano-TiO₂ ethanol colloids were obtained with strong fluorescence emission intensity around 414 nm.

Pei-sheng et al. [41] used a titanium plate with a diameter of 15 mm and thickness of 2 mm to formulate TiO₂ nanofluid by using laser ablation method while continuously stirring the plate with the help of rotator. The titanium plate was placed inside the glass vessel filled with base fluid (polyvinylpyrrolidone). To meet the experimental requirements, the laser beam was focused on the titanium plate by passing it through the quartz lens of focal length 250 mm.

Liang et al. [42] formulated TiO₂ nanofluid by placing the titanium plate into a solution of deionized water (7 cm³) and a varying quantity of surfactant (0.001 M, 0.01 M, and 0.1 M). A laser beam was focused on the dipped plate with a maximum output power of 150 mJ/pulse via a lens of focal length of 250 mm that vaporized the plate and nanoparticles were spread into the base fluid. The solution of TiO₂ prepared by adding SDS (0.01 M), endured cluster formation and remained stable for more than a week.

This is a much more reliable, cost-effective and efficient technique compared to numerous traditional time consuming and multi-step processes.

2.1.3. Submerged Arc Method

In this method, a pure titanium rod is submerged into the base fluid in the vacuum chamber. After that, the process parameters such as pulse duration, electric current breakdown voltage, off-time duration, the pressure of the vacuum chamber and base fluid temperature are established, an electric arc generator generates a high pulsed arc in the temperature range of 5000–20,000 K that evaporates the deployed titanium rod along with some base fluid. The vaporized metal particles are cooled and condensed in the vacuum chamber with the help of isolated liquid. The nanofluids prepared by using this method are stabilized and well dispersed in the base fluid.

Chang and Liu [43] analyzed the process parameters of the arc spray nanofluid synthesis system and prepared deionized water-based TiO₂ nanofluid. Nanoparticles with an average extent of less than 20 nm, high distribution, improved roundness and dispersion in the base fluid were successfully achieved by using this technique. Figure 5 shows the schematic diagram of the Chang and Liu experimental apparatus. Chang and Lin [44] used the improved submerged arc method to fabricate TiO₂ nanofluid. In this method, electric energy was converted to heat energy with temperatures exceeding 100,000 °C, which melts the metal more rapidly. By using this improved method, they produced finer, stabilized and dispersed nanoparticles as shown in Figure 6.

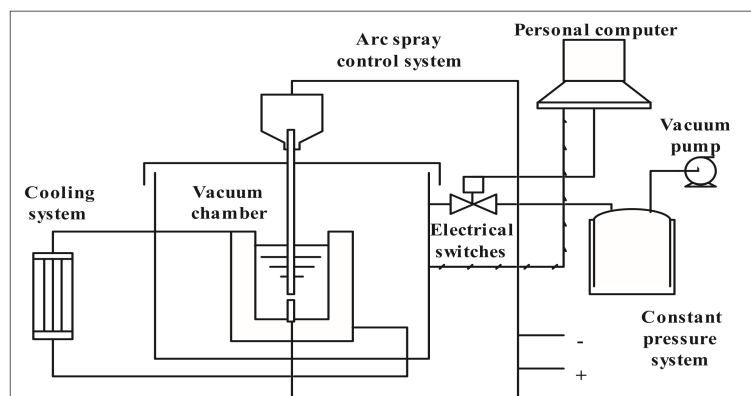


Figure 5. Schematic diagram of submerged arc method [43].

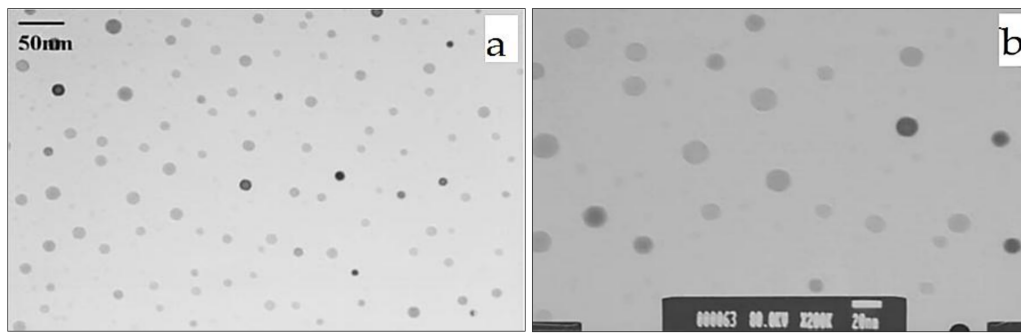


Figure 6. (a) FE-SEM image of TiO₂ nanoparticles; (b) TEM image of TiO₂ nanofluid [44].

Jwo et al. [45] fabricated TiO₂ nanofluid by using the submerged arc nanoparticles synthesis system and investigated the ultraviolet characteristics of the prepared nanocomposite. They observed that the nanocomposite of TiO₂ with UV irradiation can be more effective for the decomposition of Toluene.

Wu and Kao [46] used the arc spray nanoparticle synthesis system (ASNSS) to prepare TiO₂ nanofluid to be used as engine lubrication oil. A focused electric arc of temperature in the range of 6000 °C to 12,000 °C was used to evaporate the titanium in the vacuum chamber. The vaporized titanium was transformed into nanocrystalline powder which collected in the cooling chamber and dispersed into the ethylene glycol to acquire the final solution.

By using this technique, we can easily achieve a temperature of 10,000 °C that is more than enough to melt and vaporize the titanium rod. By employing this technique, nanofluids that are generated are highly stable with improved particle roundness and dispersion.

2.2. Two-Step Method

The most widely used method for the preparation of TiO₂ nanofluids is the two-step method in which the nanoparticles, nanotubes, nanofibers or nanorods are firstly prepared by using sol-gel methods, microemulsion, hydrothermal synthesis or any other technique. Then, the prepared nanopowder is dispersed into the base fluid with the help of ball milling, high shear mixing, ultrasonic agitation or intensive magnetic force agitation. Figure 7 illustrates the basic steps involved in a two-step method. The major benefit of using this method is the production of nanofluids on an industrial scale, on the other hand, the problem with this method is the agglomeration of particles. For this purpose, surfactants are used to avoid or reduce agglomeration/surface tension. However, this problem reinforces the use of a single step preparation method.

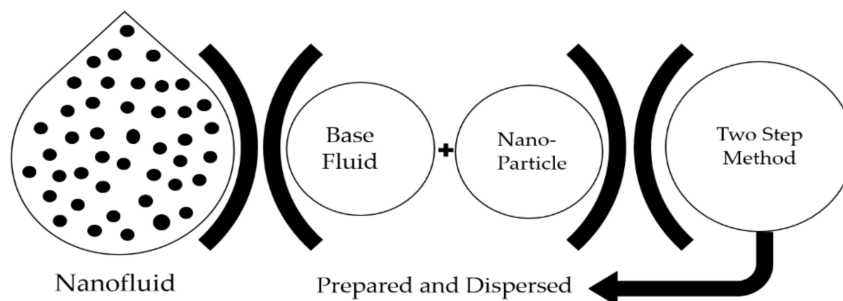


Figure 7. Two-step method.

2.2.1. Preparation of Nanoparticles

There are several routes that are commonly used for the preparation of TiO₂ nanopowder.

Sol-Gel Method

Sol-gel method is mostly used for the synthesis of nanoparticles because of its versatility in producing particles with a high surface area. Behnajady et al. [47] explained the sol-gel method very precisely and this is shown in Figure 8. They completed the whole process in four different steps; in the first step the precursor titanium is dissolved in the solvent and after that the mixture is sonicated with the help of an ultrasonic bath. Hydrolysis process is then carried out by adding the deionized water drop by drop into the prepared mixture of precursor titanium and solvent under magnetic stirring or reflux. In the final step, the obtained product, which looks like a gel, is dried and calcinated to get a crystalline powder.

Sharma et al. [48] prepared a nanocrystalline powder of TiO₂ using the sol-gel technique while using titanium tetra-isopropoxide [Ti(OCH(CH₃)₂)₄] as a precursor material. The used precursor material was added into a solution of deionized water and isopropanol at a temperature of 80 °C, after 1 h the solution of deionized water and concentrated [HNO₃] was mixed with the solution containing nanocrystalline powder in a round flask and stirred for 6 h. For proper mixing, the stirring process was not stopped during the whole process. The prepared sol-gel was heated up at 300 °C for 1 h to obtain dry nanopowder in crystalline form.

Cesnovar et al. [49] used TTIP (titanium tetra-isopropoxide) as the starting material and observed the final phase of fabricated nanocrystalline TiO₂. Experimental results showed that temperature variation has a significant effect at the intermediate state on the phase of Ti(OH)₄, TiO₂ structure changed from anatase to rutile as the temperature was increased during the calcination process. The temperature variation during the calcination process also increased the crystalline size. Vijayalakshmi and Rajendran [50] adopted the sol-gel method and prepared TiO₂ nanoparticle by dissolving titanium (IV) isopropoxide (TTIP) in absolute ethanol. Nitric acid was used during this approach to restrain the hydrolysis process and to adjust the pH value of the solution. Distilled water was also added to the molar ratio of Ti:H₂O = 1:4.

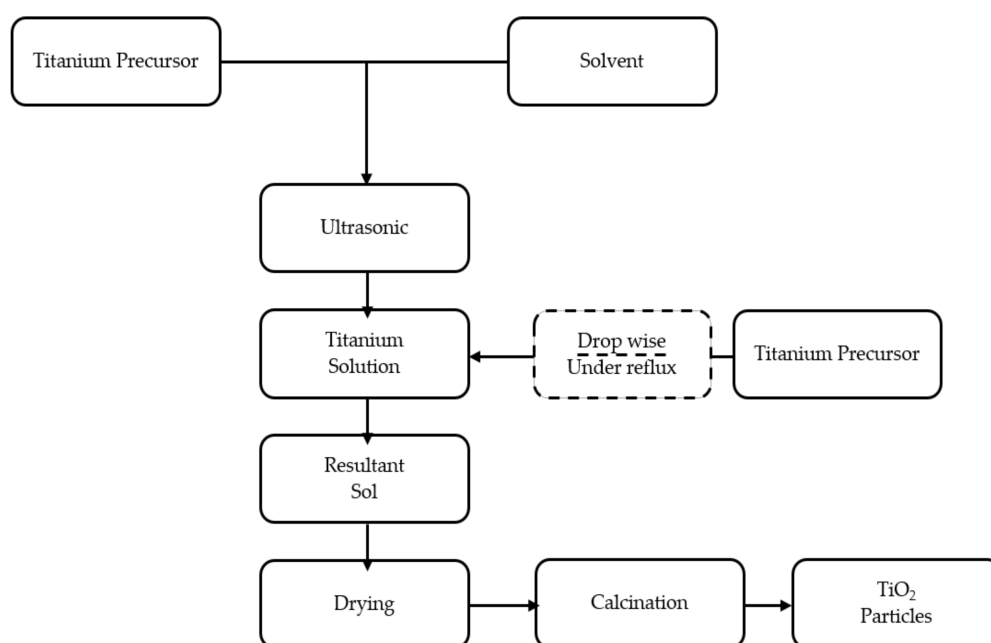


Figure 8. Steps involved in the preparation of TiO₂ nanoparticles via sol-gel [47].

The sol-gel technique has an additional advantage of controlling the reaction rate by controlling the condensation and hydrolysis using chemical means and usage of alk-oxides, as compared to the other nanoparticle fabrication techniques.

Hydrothermal Synthesis

The hydrothermal synthesis method has been utilized to synthesize single crystals from an aqueous solution in an apparatus consisting of a thin-walled steel pressure vessel (called an autoclave) at higher temperature and pressure. Zhang et al. [51] produced anatase type TiO₂ nanowires (30–45 nm) from TiO₂ nanoparticles using hydrolysis synthesis, 1-gram anatase type TiO₂ was placed inside a Teflon-lined autoclave filled with 10 M aqueous solution of NaOH. For heating and cooling purposes, the autoclave was sealed into a stainless-steel tank and heated at 200 °C for 2 h. The heated mixture was cooled down gradually to room temperature by placing it in the atmospheric air. After that, the prepared solution was washed out with distilled deionized water, HCl aqueous solution and absolute ethanol several times and dried for 6 h at 70 °C.

Suzuki and Yoshikawa [52] used the hydrothermal technique for the preparation of nanotubes by using 150 mg TiO₂ of anatase type powder as a starting material. The mixture of TiO₂ powder and an aqueous solution of NaOH was placed into a Teflon-lined stainless autoclave for 72 h at 110 °C. The precipitated powder was then washed out with distilled water and an aqueous solution of HCl after cooling it at room temperature. Finally, the powder was dried at 60 °C for 2 h.

Nian and Teng [53] observed while preparing the anatase type TiO₂ nanorods from nanotubes, that the crystal size of the particles increased by increasing the pH value of suspension. The key steps involved during the transformation of nanotubes to nanorods were the oriented attachment of crystallites and the shrinkage of tube walls. Experimental procedures involved the mixing of commercially available powder (70% anatase, 30% rutile) into the solution of 10N NaOH and placing it inside the Teflon-lined autoclave at 130 °C for 20 h. The sample was then washed out with the solution of HNO₃ by varying the amount to give different pH values. Hydrothermal treatment was carried out in an autoclave for 48 h at 175 °C, the developed slurries were then dried at 100 °C for 3 h after the process of filtration to get the final product.

Yin et al. [54] formulated anatase and rutile type phase pure TiO₂ nanocrystallites by autoclaving the amorphous TiO₂ in the presence of HF and HCl, and citric and nitric acids, respectively. The anatase type TiO₂ prepared by using HF with nitric acid as a cooperative catalyst has an irregular surface, while the particles formulated by using HCl as a cooperative catalyst gave a regular crystalline surface. Pure phase rutile TiO₂ was also obtained by autoclaving in the presence of cooperative catalysts citric and nitric acids.

Pavasupree et al. [55] studied the photocatalytic activity and found that the mesoporous anatase TiO₂ nanopowder (prepared by the hydrothermal method) showed much better results as compared to nanorods, mesoporous, nanofibers TiO₂ (prepared by sol-gel method) and commercial (P-25, JRC-03, and JRC-01) TiO₂. Distilled water of 40 mL was added to a mixture of (titanium (IV) butoxide (Aldrich, St. Louis, MO, USA) and acetylacetone) and stirred for 5 min. The obtained solution was cooled down at room temperature after heating it in the Teflon-lined stainless-steel autoclave for 1 h at 130 °C. At the final stage, the obtained solution was washed out with water and 2-propanol.

Corradi et al. [56] made a comparison of conventional and microwave hydrothermal synthesis for the preparation of TiO₂ nanopowder and found that the powder synthesized via microwave hydrothermal synthesis was more crystalline and took less time compared to the conventional one. A solution of TiOCl (0.5 M) was used as the starting material and the hydrothermal process was carried out by using a microwave at 195 °C and varying the time from 5 min to 1 h. Parameters like temperature and pressure were monitored by a computer control system. Conventional synthesis was also conducted at the same temperature but using different time intervals ranging from 5 min to 1 h. In the final stage, the suspensions from both processes were washed out with bi-distilled H₂O and NaOH solution to eliminate chloric ions and neutralize the excess acidity.

The above-discussed technique gained importance in the twenty-first century due to its many advantages, including low energy consumption, the reactions' performance in a liquid environment, low process temperature and environmental benevolence. The problems are the higher cost of the autoclave and observation of the crystals as it produces.

2.2.2. Preparation of Nanofluids

Preparation of nanofluids involves the suspension and dispersion of nanoparticles into the base fluid prepared by using the previously described techniques. It is very difficult to suspend nanoparticles uniformly and stably into the base fluid due to the presence of strong attractive van der Waals forces between them that lead to colliding and aggregation effects. So, different techniques have been used for proper dispersion of nanoparticles into the base fluid. Ultrasonication, magnetic stirring, surfactant addition and pH adjustment are the techniques used most commonly for two-step methods, with the last two techniques mostly used in combination with the first two techniques for better dispersion and stability of nanofluids.

Ultrasonication Method

Ultrasonication is the act of applying ultrasonic sound waves of frequency >20 kHz to agitate the nanoparticles into the base fluid that reduces nano-sized cluster formation by breaking intermolecular interactions.

Leena and Srinivasan [57] followed the ultrasonication path while synthesizing TiO₂ nanofluid with different concentrations of TiO₂ nanoparticles in distilled water, prepared by using the sol-gel method. Figure 9 shows the XRD pattern and HR-TEM image of the prepared sample of TiO₂ nanoparticles. The nanoparticles were dispersed in water and ultrasonicated while at room temperature, to obtain the desired solution of Titania. The ultrasonication process prevented particle agglomeration by dispersing the particles into the base fluid. Figure 10 shows the stability of nanofluid with different concentrations of nanoparticles.

Tajik et al. [58] performed experimentation to study the effect of ultrasonic quality during the fabrication of TiO₂ nanofluid on its stability and found that nanofluid prepared via continuous pulses of the ultrasonicator show high stability as compared to nanofluid prepared with discontinuous pulses. The TiO₂ nanofluids sample presented in this study were prepared by dispersing TiO₂ nanoparticles with different volume concentrations and ultrasonicated for 30 min to disperse the particles into the base fluid.

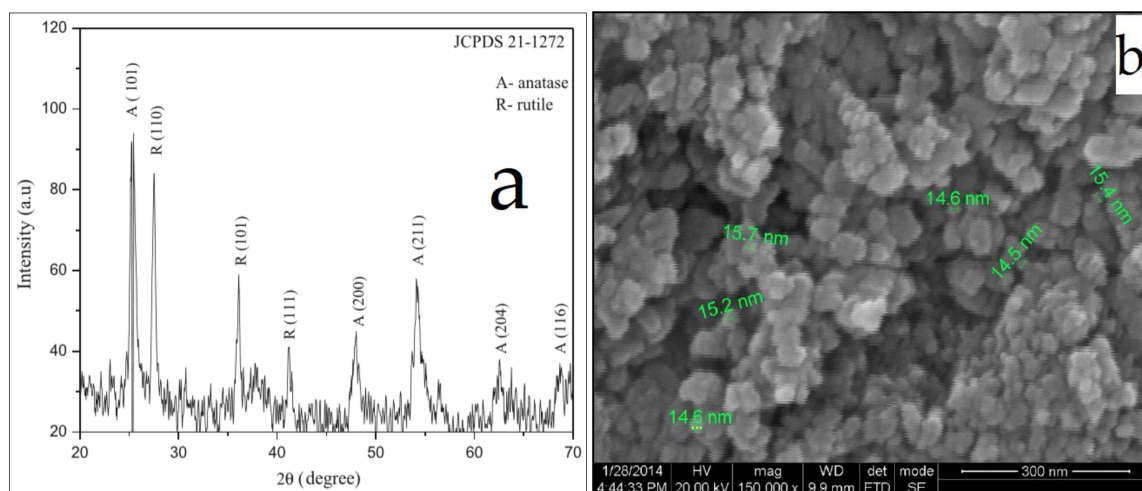


Figure 9. (a) XRD pattern of TiO₂; (b) HR-SEM morphology of TiO₂ [57].

Mo et al. [59] formulated and investigated the effects on crystallization characteristics of TiO₂ nanofluid by using rutile and brookite type nanoparticles. The results showed that, by varying the cooling rate (1.5–9.0 °C/min) for weight fractions of 0.30% and 0.70%, the rod shape (rutile TiO₂) nanofluids performed best compared to the spherical shape (anatase TiO₂) nanofluids and deionized water for ice storage systems.

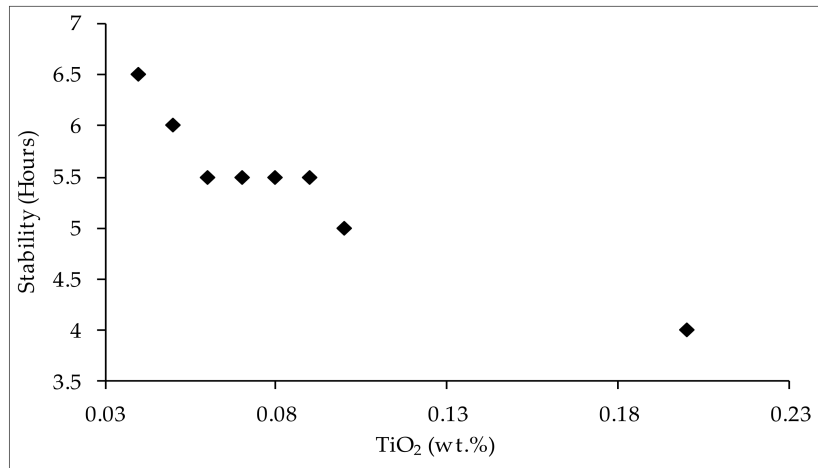


Figure 10. Leena and Srinivasan’s experimental results.

Murshed et al. [60] prepared TiO₂ nanofluid by dispersing spherical and cylindrical shaped nanoparticles in deionized water. For proper mixing of nanoparticles with different volume fraction into the base fluid, they used an ultrasonic dismembrator for 8–10 h. Experimental results showed that the thermal conductivity of the nanofluid increased with the variation of volume fraction. Palabiyik et al. [61] observed several important characteristics of the TiO₂ nanofluid that was prepared during their experiment. They found that the nanoparticle size decreased by increasing the sonication time and this decrease in size becomes stationary after reaching a specific sonification time. Figure 11 shows these results for the decrease in particle size as a function of sonication time.

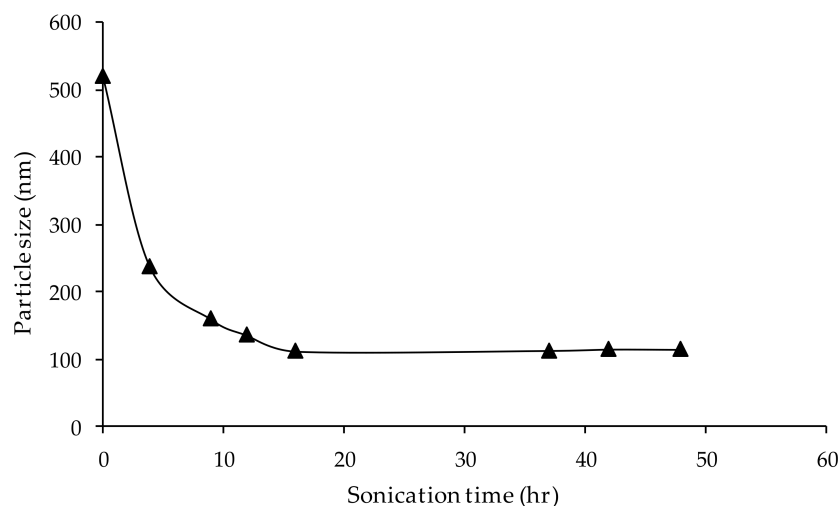


Figure 11. TiO₂ particle size as a function of ultrasonication time [61].

Tavman et al. [62] observed that the thermal conductivity of TiO₂ nanofluids was increased by increasing the concentration of the nanoparticles in the base fluid. They prepared three samples of TiO₂ nanofluids by dispersing the nanoparticles with concentrations of 0.2, 1.0, 2.0 vol. % in deionized water and ultrasonicated without adding any type of surfactant.

Shu et al. [63] prepared ethylene-glycol based nanofluid by using ultrasonication. The TiO_2 particles were submerged in the ethylene-glycol via ultrasonication and then magnetically stirred for 1 h. An enhancement in viscosity of 328 times was recorded at a volume fraction of 8.46% compared to the base fluid.

Birlik et al. [64] developed a nanofluid of TiO_2 by using sol-gel derived nanoparticles for cutting tool applications, for the purpose of using it as a lubricant during face milling 7075 aluminum alloy. Nanofluid was dispersed in the ultrasonic bath in the presence of base fluid, to confirm the stability, for more than 24 h without any noticeable agglomeration and sedimentation.

Duangthongsuk and Wongwises [65] added TiO_2 (0.2 vol. %) nanoparticle into the base fluid and investigated the heat transfer coefficient and friction factor of the prepared TiO_2 nanofluid by passing it into a horizontal double-tube counter flow heat exchanger. According to the results, the convective heat transfer coefficient was improved by about 6–10% as compared to the base fluid. Cetyltrimethylammonium bromide (CTAB) was added as a surfactant into the base fluid to ensure proper dispersion and better stability with very less concentration of about 0.01%. The desired nanofluid of Titania was then prepared by putting the nanoparticles into the base fluid and it was sonicated for 3–4 h to ensure dispersion with the help of the ultrasonicator.

Yiamsawas et al. [66] measured the viscosity of TiO_2 nanofluids prepared using an ultrasonicator at higher temperature and nanoparticle concentration and compared the viscosity variation trend that they observed by varying the particle concentration to the experimental results of several different researchers.

Turgut et al. [67] prepared TiO_2 nanofluids by enhancing the nanoparticles up to a volume of 3% and observed the relative increase in thermal conductivity and viscosity. They concluded that by varying the volume of nanoparticles, the increase in viscosity was more as compared to the increase in thermal conductivity. The nanofluids that were used during their experimental study were prepared by dispersing the nanoparticles in the deionized water and ultrasonicated with a ultrasonic vibrator to homogenize the mixture for better stability.

Kayhani et al. [68] studied the convective heat transfer coefficient and pressure drop of water-based TiO_2 by passing it through uniformly heated horizontal circular tubes and observed an increase in the heat transfer coefficient by increasing the nanofluid volume concentration. The TiO_2 nanoparticles were sonicated for 1 h at 30 °C permitting it to place groups of hydrophilic ammonium on the surface of the TiO_2 nanoparticles after mixing with 1,1,1,3,3,3 hexamethyldisilazane. Then, the prepared nanoparticles were dried and dispersed into the distilled water with a particular volume fraction. To break down the agglomerations and obtain better stability, the solution was suspended for ultrasonic vibration for 3–5 h at 400 W and 24 kHz. Figure 12 shows the Field Emission Scanning Electron Microscopic (FESEM) image of the prepared TiO_2 nanofluid.



Figure 12. FESEM image of the dispersed TiO_2 nanofluid [68].

Yoo et al. [69] found that TiO₂ nanofluid showed higher thermal conductivity as compared to the nanofluid of Al₂O₃. TiO₂ nanofluid containing 1 vol.% nanoparticles. It achieved a 14% increase in thermal conductivity which was much higher relative to the increase in the thermal conductivity of Al₂O₃. They followed the two-step ultrasonication method for the preparation of TiO₂ nanofluid, by dispersing nanoparticles into the base fluid and ultrasonicated it with pulses of 700 W at 20 kHz to prevent cluster formation and proper dispersion of nanoparticles in the base fluid.

Ultrasonication is an effective technique to overcome cluster formation by reducing the bonding forces between the particles after dispersing the powder into the base fluid. The sonication effect reduces the agglomeration effect and permits the utilization of the full potential of nanoparticles in the solution.

Magnetic Stirring

Many researchers used the magnetic stirring technique combined with ultrasonication during the preparation of nanofluids [70–72], but some used it separately to disperse nanoparticles with a low concentration. In this technique, a stir bar also called a “flea” is used to generate the stirring action. The stir bar is submerged into the solution and spins very quickly under the action of the rotating magnetic field created by stationary electromagnets or a set of rotating electromagnets underneath the vessel in a stirring apparatus.

Kavitha et al. [73] used the sol-gel method for the preparation of TiO₂ nanoparticles by using titanium tetra-isopropoxide; magnetic agitation was used for proper mixing of nanoparticles with different volume concentrations into the base fluid. The prepared nanoparticles were well dispersed in the base fluid without any settlement at the bottom of the flask. Mansour et al. [74] prepared transformer oil based TiO₂ nanofluid and used magnetic stirring for mixing of the base fluid and dispersant and then nanoparticles of titanate. They prepared six samples of nanofluid by varying the amount of dispersant (0.1–1.5 %vol.) and observed that dispersant addition played an important role in the dispersion of nanoparticles in the base fluid. Elsalamony et al. [75] used the magnetic stirrer to homogenize the mixture of SDS surfactant and distilled water before adding the TiO₂ nanoparticles into the prepared solution under ultrasonication. This technique is usually used for pre-homogenization of nanofluids and the homogenization of the mixture of surfactant and base fluid.

pH Adjustment

The dispersion environment can be adjusted by adjusting the pH value of the base fluid. This technique raises the zeta potential of the suspended nanoparticles. The significance of zeta potential is that the stability of the fluid can be directly related to the value of the zeta potential. Colloids with a higher value of zeta potential are electrically stabilized as compared to colloids with a lower value.

Li and Sun [76] investigated the effect of pH value on the sedimentation and aggregation of TiO₂ nanofluids prepared in a base fluid of (SRFA, Fe(III)). A solution of Suwannee River fulvic acid (SRFA) and Fe(III) were magnetically stirred for 1 h, after that the TiO₂ particles were dispersed in the solution of SRFA or/and Fe(III) and stirred for 24 h at a speed of 200 rpm. The stability of the experimentally prepared solution of TiO₂ nanofluids was enhanced by adjusting the pH value with the addition of 0.1 M HCl or NaOH. By using the mono-system of Fe(III) and bi-system of SRFA and Fe(III), aggregation was reduced at the pH value of 4 in the case of the mono-system and at the pH values of 6 and 8 in the case of the bi-system.

He et al. [77] mixed the nanoparticles of TiO₂ in distilled water and ultrasonicated for 30 min in order to break the agglomerations. The processed solution was then passed through the medium mill to further reduce the agglomeration size. In order to make the suspension more stable, its pH value was adjusted to 11 to prevent any type of re-agglomeration. They used this technique to produce nanofluids with 1.0%, 2.5%, and 4.9% by weight concentration.

Wen and Ding [78] carried out the pH adjustment method to stabilize the TiO₂-water nanofluid and performed studied its heat transfer performance. Figure 13 shows the variation of the zeta potential of TiO₂ nanofluid for a particle concentration of 0.024 %vol. with pH adjustment.

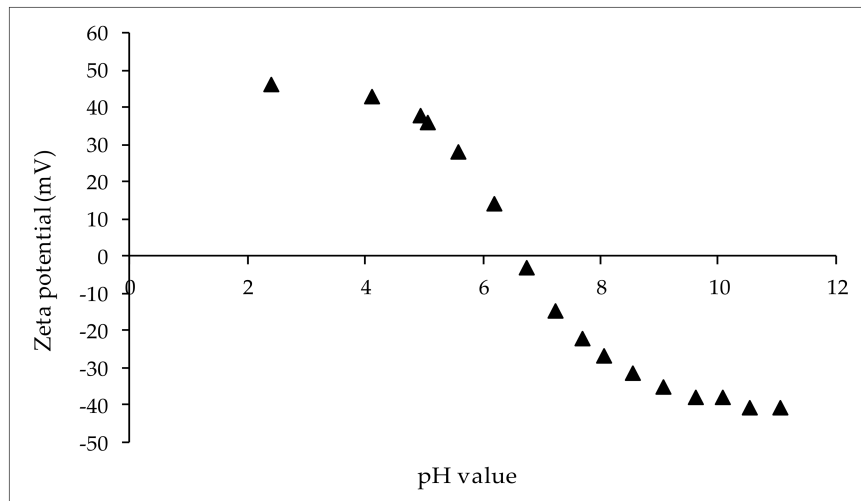


Figure 13. Zeta potential of the TiO₂ particle (0.024 %vol.) in distilled water [78].

Some other related studies that have been carried out with pH adjustment of the formulated solution will be discussed in the combination usage section because it is an additional process proven to improve the stability of nanofluids.

Combination Usage

Combination usage involves the utilization of a combination of different processes such as ultrasonication, magnetic stirring, and adjusting pH value of the base fluid to accomplish nanofluids with better dispersion efficiency and stability. Wei et al. [79] used a combination of magnetic stirring and ultrasonication techniques for the preparation of TiO₂ nanofluid with different concentrations by using diathermic oil (0.86 g/cm³, −10–320 °C) as the base fluid. Figure 14 shows the transmission electron microscope (TEM) image of the dried nanoparticles.

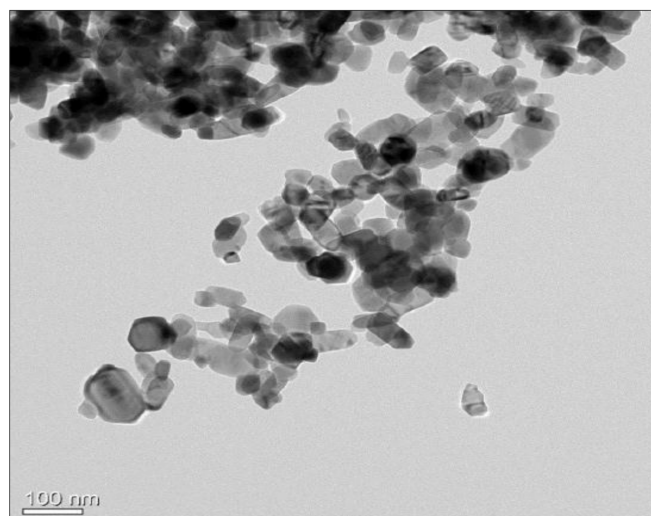


Figure 14. TEM image of the dried TiO₂ nanoparticle [79].

The process involved the dispersion of anatase type TiO_2 nanoparticles into the base fluid, adding oleic acid as a surfactant to increase the stability of the solution, stirred magnetically at 500 rpm and ultrasonicated for 1 h to homogenize the mixture at room temperature. The diameter of the particles just after the experiment was 22 nm and 19.3 nm with 0.4 vol. % and 0.2 vol. %, respectively, but increased to 48.5 nm when measured after 10 days.

Shao et al. [80] compared the stability of the TiO_2 - H_2O binary nanofluids prepared by using titanium dioxide nanotubes (TiNTs) and titanium dioxide nanosheets (TiNSs) and found that the stability of nanofluid improved by using a combination of TiNTs and TiNSs powder rather than the usage of a single powder of TiNTs or TiNSs with the same concentration. They got the desired binary nanofluids by adding the mixed powder of TiNTs and TiNSs into the base fluid and stirred up to 30 min using the magnetic stirrer to ensure better suspension of powder into the base fluid. To get a more stable solution, ultrasonic agitation was performed with the help of ultrasonic cleaner for 1 h.

Khosravifard et al. [81] dispersed TiO_2 -CNTs nanocomposite powder into a mixture of water and propylene (50:50), stirred and agitated thoroughly for 30 min to synthesize the desired TiO_2 -CNTs nanofluid. The thermal conductivity of all samples was measured by using the apparatus (H471) and the study concluded that there was an intensive increase in thermal conductivity with a temperature below 28 °C, after that, it increased linearly with temperature.

Jarahnejad et al. [82] investigated the effect of temperature, size of nanoparticles, the addition of surfactants and concentration on the dynamic viscosity of water-based TiO_2 . The nanofluids of TiO_2 were formulated by using a two-step method and stabilized by adding polycarboxylate and tri-oxadecane acid, adjusting pH value and dispersing the nanoparticles into the base fluid while sonicated. Ghadimi and Metselaar [83] revealed that nanofluid prepared with a low concentration of TiO_2 nanoparticles and sodium dodecyl sulfate (SDS) surfactant (0.1 wt. %) showed greater thermal conductivity along with the highest stability. Nanofluid preparation involved the mixing of base fluid and surfactant with the help of a magnetic stirrer and it was ultrasonicated while adding the nanoparticles for proper dispersion. Hussein et al. [84] used magnetic stirring and ultrasonication to prepare a homogeneously dispersed solution of TiO_2 . The experimental results showed an increase in viscosity and thermal conductivity of Titania by increasing the volume concentration of nanoparticles.

Batmunkh et al. [85] improved the thermal conductivity of TiO_2 nanofluid with the addition of small amounts of nanoparticles of modified silver (Ag). Firstly, the composite of TiO_2 was prepared by using the combination of small (70%) and large nanoparticle (30%) with the help of a mechanical stirrer. For the purpose of doing a comparison, they prepared the three samples of nanofluids with 1, 2 and 3 wt. % concentration of nanocomposite particles mixed with flattened Ag nanoparticles and dispersed into water. To avoid cluster formation, the mixing process was carried out with the help of an ultrasonicator for 1 h in order to get better dispersion of nanoparticles in nanofluid. Bahiraei et al. [86] assessed the viscosity variation against temperature and nanoparticle volume concentration of the TiO_2 nanofluid formulated by a two-step method using the combination of both magnetic stirring and ultrasonication, respectively. The prepared nanofluid was stable for several months, without exhibiting any indication of particle precipitation and agglomeration. Arani and Amani [87] studied the effect of nanoparticle size and concentration on pressure drop and Nusselt number of the flowing nanofluid inside the counter flow heat exchanger and found an increase in Nusselt number and a power drop by increasing the Reynolds number. They also found that nanoparticles of diameter 20 nm performed best and achieved greater heat transfer rate. An ultrasonic vibrator (up to 3 h) and cetyl trimethyl ammonium bromide (0.01 %vol.) as a surfactant were used to avoid cluster formation and ensure better stability. Figure 15 shows the TEM image of TiO_2 nanofluids with dispersion of nanoparticles of different sizes.

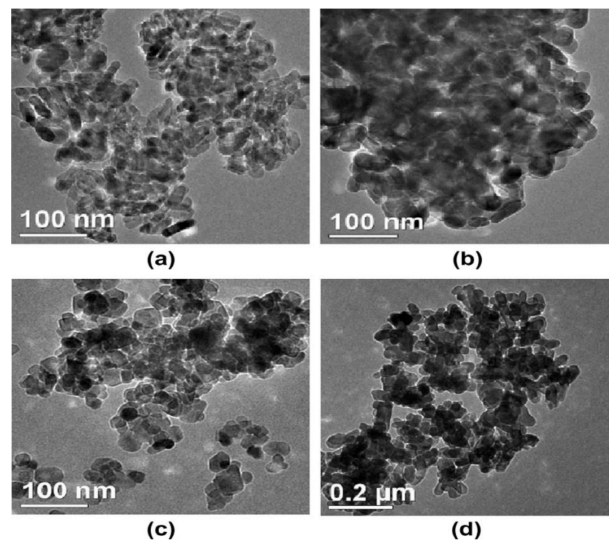


Figure 15. TEM image of the TiO₂ nanofluids with dispersed nanoparticles of average diameter. (a) 10 nm (b) 20 nm (c) 30 nm (d) 50 nm [87].

Vakili et al. [88] compared the convection heat transfer coefficients of the TiO₂ nanofluids prepared by using distilled water and a combination of distilled water and ethylene glycol as the base fluid and found that the value of the convection heat transfer coefficient was more when they used the combination of water and ethylene glycol. The TiO₂ nanoparticles and base fluid were transferred into the ultrasonic vibrator and sonicated for 4 h, a solution of NaOH was also added to the suspension to adjust its pH value to avoid agglomeration due to cluster formation.

In order to get better dispersion of nanoparticles with less agglomeration, upgraded thermophysical properties, and improved stability, most researchers prefer the combination of magnetic stirring and ultrasonication to break down the clusters and pH adjustment to acquire stable nanofluids.

3. Thermal Conductivity

The thermal conductivity of the nanofluids has been measured by using different classical models, including the Hamilton and Crosser [89] model.

$$k_{eff} = k_{bf} \left[\frac{k_{np} + (n - 1)k_{bf} - (n - 1)\varphi(k_{bf} - k_{np})}{k_{np} + (n - 1)k_{bf} + \varphi(k_{bf} - k_{np})} \right] \tag{2}$$

where $n = \frac{3}{\omega}$ in which n and ω represent the empirical shape factor and sphericity respectively. The factor ω is defined as the ratio of the surface area of a sphere (equal in volume of the given particle) to the surface area of the particle. For nanofluids in which the thermal conductivity of nanoparticles is larger than a factor of 100, the above equation should be used for the value of n and for all other nanofluids n may be taken as 3. The H-C (Hamilton and Crosser) model is an improved form of the Maxwell model [1] that was used to predict the thermal conductivity of well dispersed solutions of solid-liquid at low volume concentration of nanoparticles. The Maxwell model considered the thermal conductivity and volume concentration of the base fluid and nanoparticles while the H-C model also considers the effects of particles shape. Equation (3) represents the Maxwell model used to compute the thermal conductivity of nanofluids.

$$k_{eff} = k_{bf} \left[\frac{k_{np} + 2k_{bf} + 2\varphi(k_{np} - k_{bf})}{k_{np} + 2k_{bf} - \varphi(k_{np} - k_{bf})} \right] \tag{3}$$

The H-C model is used for cylindrical and spherical particles and the Maxwell model is used only for spherical particles.

Nan et al. [90] generalized the Maxwell model by introducing the influence of interfacial thermal resistance with particle shape, size, and orientation. The prescribed model for spherical particles is expressed by:

$$k_{eff} = k_{bf} \left[\frac{2k_{bf} + (1 + 2\alpha)k_{np} + 2\varphi \left[(1 - \alpha)k_{np} - k_{bf} \right]}{2k_{bf} + (1 + 2\alpha)k_{np} - \varphi \left[(1 - \alpha)k_{np} - k_{bf} \right]} \right] \tag{4}$$

In this expression the dimensionless parameter α describes the particle-fluid interaction and is expressed as follows:

$$\alpha = \frac{Rk_{bf}}{r_{np}}$$

where R is the thermal boundary resistance coefficient, and r represents the radius of the dispersed nanoparticle.

The limitation of the particle volume fraction can be avoided by using the Bruggeman model [91] used for a binary mixture of randomly dispersed homogeneous spherical nanoparticles.

$$k_{eff} = \frac{k_{bf}}{4} \left[(3\varphi - 1) \frac{k_{np}}{k_{bf}} + (2 - 3\varphi) + \frac{k_{bf}}{4} \sqrt{\Delta} \right] \tag{5}$$

$$\Delta = \left[(3\varphi - 1)^2 \left(\frac{k_{np}}{k_{bf}} \right) + (2 - 3\varphi)^2 + 2(2 + 9\varphi^2) \left(\frac{k_{np}}{k_{bf}} \right) \right]$$

The updated H-C model is the Wasp model [92], most commonly used for convection heat transfer problems established by considering the unity empirical shape factor.

$$k_{eff} = k_{bf} \left[\frac{k_{np} + 2k_{bf} - 2\varphi(k_{bf} - k_{np})}{k_{np} + 2k_{bf} + \varphi(k_{bf} - k_{np})} \right] \tag{6}$$

The discussed classical models were unable to get the exact value of thermal conductivity for nanofluids because these models do not consider the effect of temperature, size of the particle, particle distribution, interfacial layer, cluster formation and Brownian motion of particles.

Xie et al. [93] considered the effects of nanolayer thickness, volume fraction, nanoparticle size and thermal conductivity ratio of the nanoparticle to the base fluid in the derived model to measure the enhanced thermal conductivity of nanofluids. Equation (7) represents the Xie thermal conductivity model.

$$k_{eff} = 1 + 3\Theta \varphi_T + \frac{3\Theta^2 \varphi_T^2}{1 - \Theta \varphi_T} \tag{7}$$

$$\Theta = \frac{\beta_{lf} \left[(1 + \gamma)^3 - \beta_{pl} / \beta_{fl} \right]}{(1 + \gamma)^3 + 2\beta_{lf} / \beta_{pl}} \quad \therefore \gamma = \frac{\delta}{r_p}$$

$$\beta_{lf} = \frac{k_l - k_f}{k_l + 2k_f} \quad \beta_{pl} = \frac{k_p - k_l}{k_p + 2k_l} \quad \beta_{fl} = \frac{k_f - k_l}{k_f + 2k_l}$$

where δ and r_p represent the nanolayer thickness and particle radius, respectively and γ is the ratio between them.

Researchers derived different theoretical models by considering different parameters to estimate the thermal conductivity of nanofluids. Table 1 presents the final states of some derived models with a brief discussion.

Table 1. Thermal conductivity models.

Researcher	Derived Model	Discussion
Yu and Choi et al. [94]	$k_{eff} = k_{bf} \left[\frac{k_{pe} + 2k_{bf} + 2(k_{pe} - k_{bf})(1 + \beta)^3 \varphi}{k_{pe} + 2k_{bf} - (k_{pe} - k_{bf})(1 + \beta)^3 \varphi} \right]$ $k_{pe} = k_p \left[\frac{2(1 - \gamma) + (1 + \beta)^3(1 + 2\gamma)\gamma}{-(1 - \gamma) + (1 + \beta)^3(1 + 2\gamma)} \right]$	Modified Maxwell model and included nanolayer thickness
Wang et al. [95]	$k_{eff} = k_{bf} \left[1 + \frac{\frac{3\varphi(\rho_p)}{\rho_f}}{1 - \frac{3\varphi(\rho_p)}{\rho_f}} \right]$	The developed comprehensive model included the nanolayer thickness, particle size, temperature, volume fraction and the interaction between adjacent nanoparticles.
Chandrasekar et al. [96]	Model I: $k_{nf} = k_{bf} \left[\left(\frac{c_{p,nf}}{c_p} \right) \left(\frac{\rho_{nf}}{\rho} \right)^{1.33} \left(\frac{M}{M_{nf}} \right)^{0.33} \right]$ Model II: $k_{nf} = k_{bf} \left[\frac{k_p + (n-1)k_{bf} + (n-1)(k_p - k_{bf})(1 + \beta)^3 \varphi}{k_p + (n-1)k_{bf} - (k_p - k_{bf})(1 + \beta)^3 \varphi} \right]$	Model I used to determine the thermal conductivity of nanofluid over a large range of particle concentration, size and different base fluids and particle materials. Model II helped to visualize the percentage contribution of layer thickness, particle shape, Brownian motion to the enhancement in thermal conductivity of nanofluids.
Avsec et al. [97]	$k_{nf} = k_{bf} \left[\frac{k_p + (n-1)k_{bf} - (n-1)(k_p - k_{bf})\varphi_{eff}}{k_p + (n-1)k_{bf} + (k_p - k_{bf})\varphi_{eff}} \right]$ $\varphi_{eff} = \varphi \left(1 + \frac{h}{r} \right)^3$	Considered the liquid layer thickness, thermal conductivities of base fluid and nanoparticles but not the interface between particles and particle size.
Corcione [98]	$k_{nf} = 1 + 4.4Re^{0.4}Pr^{0.66} \left(\frac{T}{T_{ref}} \right)^{10} \left(\frac{k_p}{k_{bf}} \right)^{0.03} \varphi^{0.66}$	The empirical correlation of Corcione is applicable with 1.86% of standard deviation error over a wide range of temperature (294–324 K), nanoparticle diameter (10–150 nm) and volume fraction (0.002–0.9)

The experimental results from different studies has shown that the thermal conductivity of TiO₂ nanofluids increases by increasing the volume concentration of nanoparticles but no one has clarified the upper limit or extent to which nanofluids follow this increasing trend [60,99–104].

Figure 16 shows the variation in thermal conductivity as a function of temperature. The error bars are used to present the information regarding the effect of particle concentration on thermal conductivity. The upper and lower ends of the error bars show the maximum and minimum values of thermal conductivity, respectively, at the highest and lowest particle concentration used during the experimental work of different researchers.

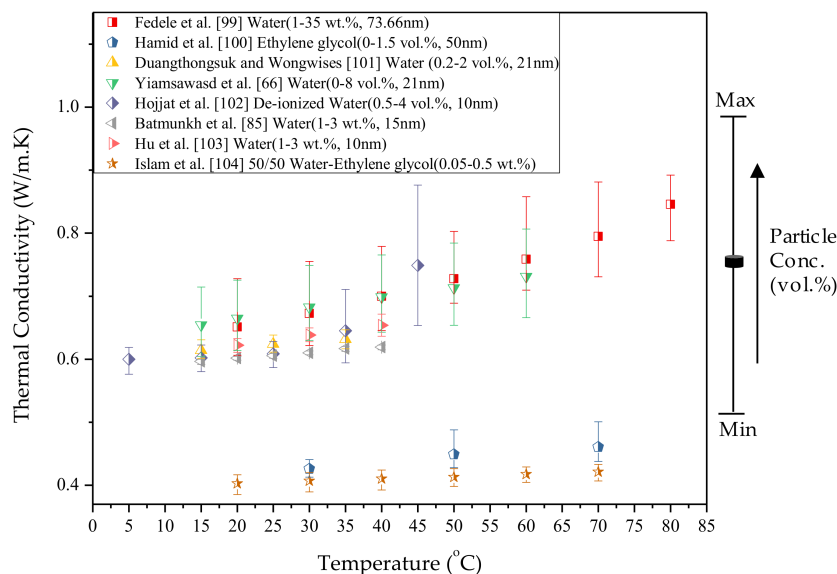


Figure 16. Thermal conductivity of TiO₂ nanofluid as a function of temperature from various studies.

Thermal conductivity depends upon various factors, mainly temperature, particle concentration, and the type of base fluid contemporarily. So, the concept of thermal conductivity variation with particle concentration is more clearly drawn in Figure 17. In this Figure, the effect of temperature is

represented with the help of error bars. The upper and lower ends relatively show the maximum and minimum values of thermal conductivity against temperature values. From all of the above discussion following deductions can be drawn:

- Thermal conductivity of TiO₂ nanofluids is directly related to the temperature.
- The variation in particle concentration directly influences the thermal conductivity of the nanofluid.
- The results obtained in different studies by using water as a base fluid showed better performance as compared to the ethylene glycol.

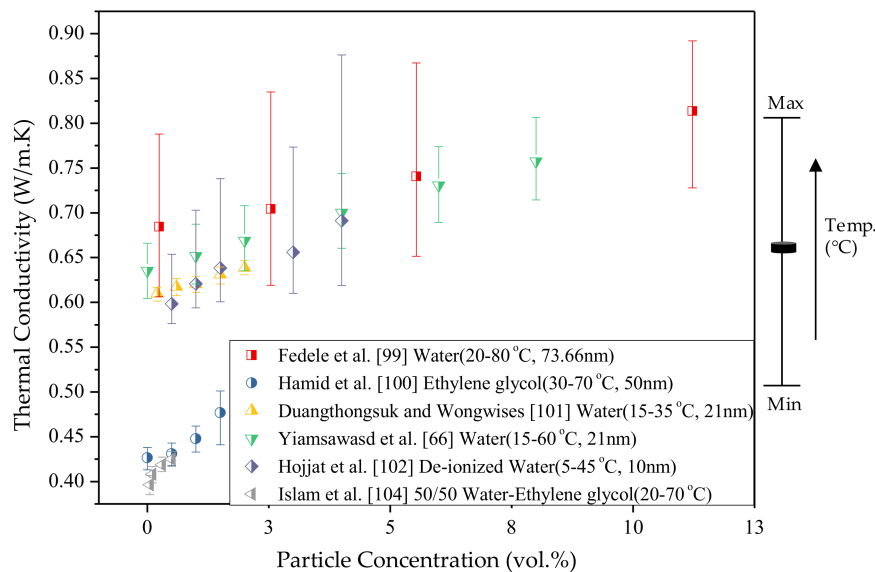


Figure 17. Thermal conductivity of TiO₂ nanofluid as a function of particle concentration (various studies).

4. Viscosity

Earlier research has been carried out to enhance the thermal conductivity of nanofluids, but it is not the only parameter that affects the heat transfer. To implement nanofluids in practical heat transfer applications, viscosity is another property that requires great attention. Factors such as pumping power [105], convection heat transfer and pressure drop [87,106] in laminar flow are greatly influenced by the viscosity of nanofluids, hence a brief review on viscosity is discussed in this literature.

The viscosity of the nanofluid depends on the quantity and effects of different parameters such as nanoparticle volume fraction [2,67,86,105,107], base fluid, particle size [83], nanolayer thickness, particle shape, dispersion technique, pH value, temperature [66,83,86,105], the effect of clustering and Brownian motion of nanoparticles. Different instruments, like a viscometer, rheometer etc. have been used to measure the viscosity of nanofluids and the measured data has been compared to well-known correlations, which are discussed below.

Einstein [108] developed the first model to measure the viscosity of nanofluids in 1906. The spherical shape of nanoparticles and less volume fraction ($\varphi < 0.02\%$) were the factors that limited the formulated model of Einstein. Moreover, the discussed model did not consider the structure and particle to particle interaction within the solution.

$$\mu_{nf} = (1 + 2.5\varphi)\mu_{bf} \tag{8}$$

In 1952, Brinkman [109] extended the work of Einstein by reducing the limitations of nanoparticles volume concentration to some extent. The developed model of Brinkman was more effective and

acceptable for volume fractions less than 4%. Equation 9 represents the empirical formula of Brinkman’s model.

$$\mu_{nf} = \frac{\mu_{bf}}{(1 - \varphi)^{2.5}} \tag{9}$$

Batchelor’s [110] model considered the effect of Brownian motion of the spherical nanoparticles and introduced the new model by modifying the Einstein equation. The correlation of this developed model is expressed as:

$$\mu_{nf} = (1 + 2.5\varphi + 6.2\varphi^2)\mu_{bf} \tag{10}$$

Nelson [111] proposed his power law model in 1970 which was considered more appropriate for nanoparticles more than 2% by volume fraction. Equation (11) denotes the Nelson model.

$$\mu_{nf} = \left[(1 + 1.5\varphi)e^{\frac{\varphi p}{(1-\varphi_m)}} \right] \mu_{bf} \tag{11}$$

where φ_m and φ_p represent the maximum volume fraction and nanoparticles volume concentration, respectively.

The above models were outdated and failed to show reasonable agreement with the experimental results for higher concentrations of nanoparticles (above 1 %vol.) [66,101,104], because these models considered the viscosity of nanofluid as a function of particle concentration and base fluid viscosity only and did not consider the effect of temperature, which has a strong connection with viscosity [66, 83,86,105,112]. However, the effect of temperature on the viscosity of TiO₂ is contradictory according to some reports [113,114]. More recently, researchers have worked to develop more accurate models by introducing different parameters and factors, these are outlined in Table 2.

Table 2. Viscosity models for TiO₂ nanofluids.

Researcher	Derived Model	Discussion																
Yiamsawas et al. [66]	$\mu_{nf} = A\varphi^B T^C \mu_{bf}^D$ A = 0.837931, B = 0.188264, C = 0.089069 and D = 1.100945	Presented correlation considered the effect of volume fraction, temperature, and viscosity of the base fluid. Where A, B, C, and D represented the correlation coefficients used to predict the viscosity.																
Corcione [97]	$\mu_{nf} = \left[\frac{1}{1 - 34.87 \left(\frac{d_p}{r_f}\right)^{-0.3} \varphi^{1.03}} \right] \mu_{bf}$ $d_p = 0.1 \left(\frac{6M}{N\pi\rho_{bf}}\right)^{\frac{1}{3}}$ where ρ_{bf} denotes the mass density of base fluid at 293 K.	This model provides the results with a 1.84% of the standard deviation of error and appropriate within the following boundaries for, temperature (293–323 K), nanoparticle diameter (25–200 nm) and volume fraction (0.0001–0.071).																
Duangthongsuk and Wongwises [101]	$\mu_{nf} = (a + b\varphi + c\varphi^2)\mu_{bf}$ <table border="1" style="margin-left: auto; margin-right: auto;"> <thead> <tr> <th>T (°C)</th> <th>a</th> <th>b</th> <th>c</th> </tr> </thead> <tbody> <tr> <td>15</td> <td>1.0226</td> <td>0.0477</td> <td>-0.0112</td> </tr> <tr> <td>25</td> <td>1.013</td> <td>0.092</td> <td>-0.015</td> </tr> <tr> <td>35</td> <td>1.018</td> <td>0.112</td> <td>-0.0177</td> </tr> </tbody> </table>	T (°C)	a	b	c	15	1.0226	0.0477	-0.0112	25	1.013	0.092	-0.015	35	1.018	0.112	-0.0177	The suggested model provided reasonable agreement with experimental results for TiO ₂ nanofluid between the temperature range (15–35 °C) and volume concentration (0.2–2.0 % vol.).
T (°C)	a	b	c															
15	1.0226	0.0477	-0.0112															
25	1.013	0.092	-0.015															
35	1.018	0.112	-0.0177															
Tseng and Lin [115]	$\mu_{nf} = (13.47 e^{35.98\varphi})\mu_{bf}$	The developed model used for TiO ₂ nanofluid when the solution is prepared by suspending the nanoparticles in distilled water with concentration (0.05–0.12)% and correlation factor R ² = 0.98.																
Chevalier et al. [116]	$\mu_{nf} = \mu_{bf} \left[1 - \frac{\varphi}{\varphi_m} \left(\frac{d}{D_a}\right)^{1.2} \right]^{-2}$ where φ = particle concentration; D_a = average diameter of aggregates; φ_m = crowding factor ($\varphi_m \approx 0.65$) in case of random packing of spheres; d = diameter of suspended particles	The presented model used in case of spherically shaped dispersants, nanofluids with high shear rate and showed Newtonian behaviour.																

Figures 18 and 19 shows the variation in viscosity as a function of temperature and particle concentration [66,67,82,99–101,105,112,117,118], respectively. In Figure 18 the error bars represent the upper and lower values of viscosity with particle concentration at the specific temperature, while in Figure 19 the ends of the bars showed the maximum and minimum values of viscosity with temperature at the specific value of particle concentration, for the particular study.

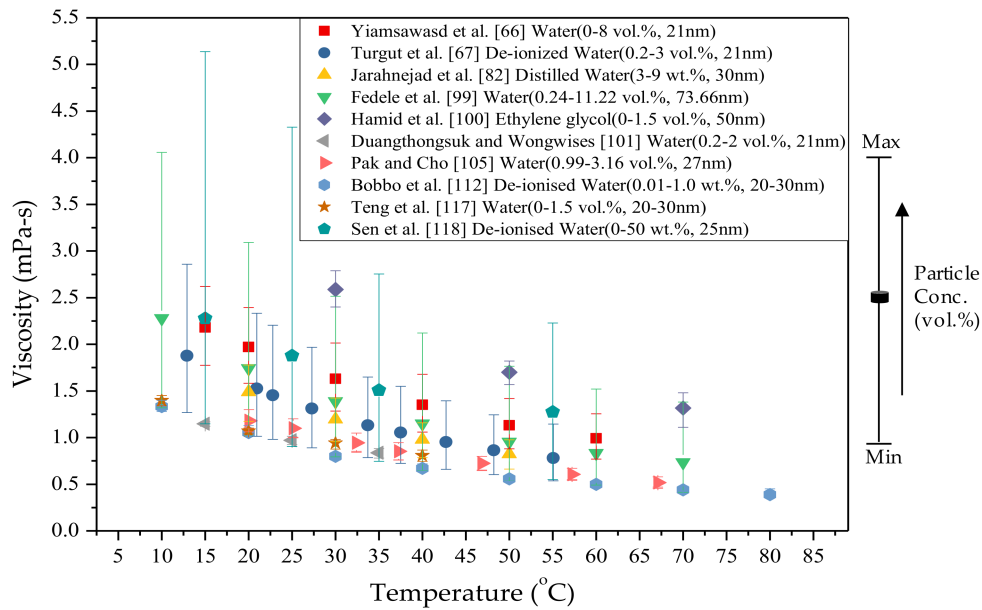


Figure 18. Viscosity of TiO₂ nanofluid as a function of temperature [Various studies].

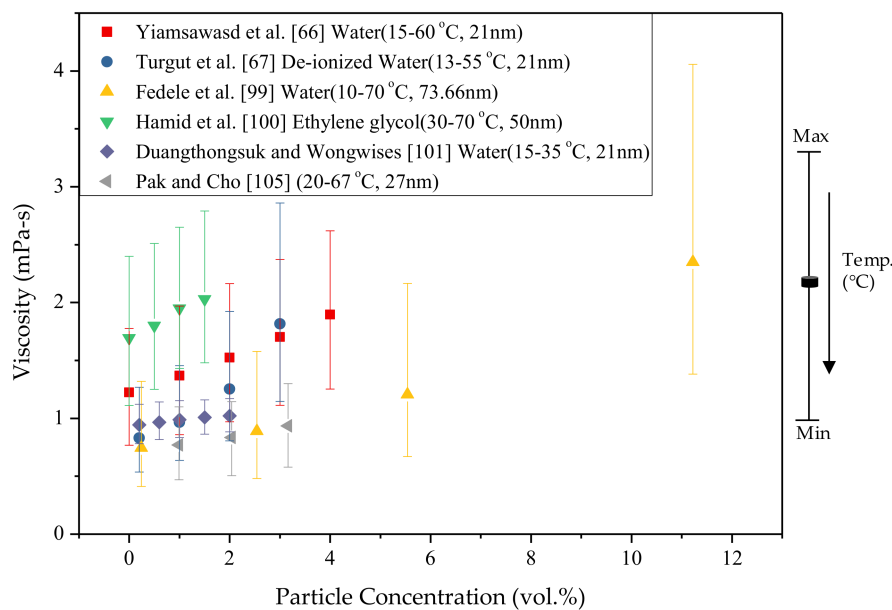


Figure 19. Viscosity of TiO₂ nanofluid as a function of nanoparticle concentration (various studies).

The studies on viscosity confirm the following points regarding viscosity variation:

- The viscosity of nanofluids shows an inverse relationship with the temperature.
- Particle concentration directly influences the viscosity of the nanofluid and shows a direct relationship with it.

5. Conclusions

This review focused on the various techniques used for the preparation of TiO₂ nanofluids. It can be concluded that although a lot of different techniques have been developed for the formulation of nanofluids, advancement faces numerous challenges. Preparation cost, particle settlement into the base fluid, surface tension, experimental environment, and erosion are problems that need

to be focused on for further enhancement of existing techniques. Instead, we can achieve better dispersion in single step methods by omitting several processes that are involved in the two-step methods. Many researchers used two-step methods because of restrictions such as a special solution environment, production of by-products, the quantity of the desired fluid, etc. On the other hand, the dispersion stability of nanoparticles in the base fluid can be achieved in two-step methods by adjusting the pH value, adding surfactant or using physical means like sonication and stirring on their own or in combination for a limited time period. Finally, we discussed two important thermophysical properties (thermal conductivity and viscosity) and their relationship with temperature and nanoparticle concentration by considering the studies of many different researchers, because the performance of nanofluids is largely influenced by these parameters.

Acknowledgments: The corresponding author wishes to acknowledge the financial support provided by the University of Engineering and Technology, Taxila, Pakistan under the faculty research project through approval letter No. UET/ASR&TD/RG-1001.

Author Contributions: H.M.A. selected topic and supervised the progress of whole work. H.B. executed critical literature review and structured the article. T.R.S., M.U.S., M.A.Q. and S.J. wrote discussions of different sections/subsections, formulated the abstract, introduction and conclusions.

Conflicts of Interest: The authors declare no conflict of interest.

Nomenclature

Abbreviations

DSC	Differential Scanning Calorimetry
ESCA	Electron Spectroscopy for Chemical Analysis
FESEM	Field Emission Scanning Electron Microscope
FETEM	Field Emission Transmission Electron Microscopy
FS	Fluorescence Spectrum
FTIR	Fourier-transform Infrared
HRSEM	High Resolution Scanning Electron Microscopy
HRTEM	High Resolution Transmission Electron Microscopy
OTS	Optical Transmission Spectroscopy
PLA	Pulsed Laser Ablation
SDS	Sodium Dodecyl Sulfate
SEM	Scanning Electron Microscope
SRFA	Suwannee River Fulvic Acid
TEM	Transmission Electron Microscopy
UV-vis	Ultraviolet-visible Spectroscopy
XPS	X-ray Photoelectron Spectroscopy
XRD	X-ray Diffraction

Symbols

c_p	specific heat capacity
D	Diameter
F	Nanolayer
H	liquid layer thickness
K	thermal conductivity
M	molecular weight
N	empirical shape factor, $3/\omega$
N	Avogadro number
P	dipole moment of spheres for a transverse
p_o	thermal dipole
Pr	Prandtl number
Q	dipole factor

Re	Reynolds number
T	Temperature

Greek Symbols

ρ	Density
φ	volume fraction
B	the ratio of nanolayer thickness to particle radius
Γ	ratio between nanolayer and particle thermal conductivity
μ	Viscosity
ρ	mass density

Subscripts

Bf	base fluid
eff	Effective
F	Fluid
fre	Freezing
L	Liquid
Nf	Nanofluid
np	Nanoparticle
p	Particle
Pe	equivalent particle
T	Total

Appendix A

Table A1. Summary of the related studies of preparation of TiO₂ nanofluids by using different techniques and methods.

Researcher	Method	Technique	Crystalline Size	Base Fluid	Surfactant	Mineral Form	Nanoparticle Loading	Characterizing Techniques
Lee et al. [39]	Single Step	Pulsed Wire Evaporation	<100 nm	Ethylene-Glycol	–	–	0.5~5.5 (vol. %)	XRD, HRTEM
Huang and Zhang [40]	One Step	Pulsed Laser Ablation	–	Anhydrous Ethanol	–	Anatase	–	TEM, UV-vis, FS
Pei-sheng et al. [41]	Single Step	Laser Ablation	35 nm	poly-(vinylpyrrolidone)	–	Rutile	–	TEM, XRD, XPS
Liang et al. [42]	Single Step	Laser Ablation	∅3 nm	Deionized Water	SDS	Anatase	–	TEM, XRD, OTS
Chang and Liu [43]	Single Step	Submerged Arc	<20 nm	Deionized Water	–	Anatase	–	XRD, TEM
Chang and Lin [44]	Single Step	Submerged Arc	10 nm	Deionized Water	–	Anatase	–	XRD, TEM, Zeta Potential
Jwo et al. [45]	Single Step	Submerged Arc	10 nm	Deionized Water	–	Anatase	–	FESEM, TEM, ESCA
Wu and Kao [46]	One Step	Submerged Arc	59 nm	Ethylene- glycol	–	–	0.1 (vol. %)	TEM
Leena and Srinivasan [57]	Two Step	Ultrasonication	~34 nm	Distilled Water	–	Anatase, Rutile	0.04–0.01, 0.2 (wt. %)	XRD, UV-vis, FS, HRSEM
Tajik et al. [58]	Two Step	Ultrasonication	30–40 nm	Distilled Water	–	–	0.005, 0.15, 0.2 (vol. %)	SEM
Mo et al. [59]	Two Step	Ultrasonication	(∅20 nm × 50 nm) and ∅15	Deionized Water	SDS	Rutile, Anatase	0.05, 0.30, 0.70 (wt. %)	TEM, DSC
Murshed et al. [60]	Two Step	Ultrasonication	(∅10 nm × 40 nm) and ∅15	Deionized Water	CTAB, Oleic acid	–	0.5–5 (vol. %)	TEM
Tavman et al. [62]	Two Step	Ultrasonication	∅21 nm	De-ionized Water	–	–	0.2, 1.0, 2.0 (vol. %)	–
Shu et al. [63]	Two Step	Ultrasonication	40–200 nm	Ethylene-Glycol	–	Anatase	0.05–35 (wt. %)	TEM, XRD, FETEM
Birlik et al. [64]	Two Step	Ultrasonication	500 nm	Deionized Water	–	Anatase	–	XRD
Duangthongsuk and Wongwises [65]	Two Step	Ultrasonication	∅21 nm	Water	CTAB	–	0.2 (vol. %)	TEM
Yiamsawas et al. [66]	Two Step	Ultrasonication	21 nm	Water	–	–	1–8 (vol. %)	–
Turgut et al. [67]	Two Step	Ultrasonication	∅21 nm	De-ionized Water	–	–	2–3 (vol. %)	–
Kayhani et al. [68]	Two Step	Ultrasonication	∅15 nm	Distilled Water	–	–	0.1, 0.5, 1.0, 1.5, 2.0 (vol. %)	FESEM
Yoo et al. [69]	Two Step	Ultrasonication	25 nm	De-ionized Water	–	–	0.1, 0.5, 1.0 (vol. %)	TEM, XRD

Table A1. Cont.

Researcher	Method	Technique	Crystalline Size	Base Fluid	Surfactant	Mineral Form	Nanoparticle Loading	Characterizing Techniques
Mansour et al. [74]	Two Step	Magnetic Stirring + Ultrasonication	>100 nm	Transformer Oil	CTAB	–	1.0, 1.5, 2.0 (vol. %)	–
Li and sun [76]	Two Step	Magnetic Stirring + pH adjustment	–	SRFA, Fe(III)	–	–	50 mg/L	Zeta potential, TEM, FTIR, XPS UV-vis
He et al. [77]	Two Step	Ultrasonication + pH Adjustment	95 nm	Distilled Water	–	Anatase, Rutile	1, 2.5, 4.9 (wt. %)	TEM, XRD
Wei et al. [79]	Two Step	Magnetic Stirring + Ultrasonication	Ø19.3, 22.2 nm	Diathermic Oil	Oleic Acid	Anatase	(0.1–1 (vol. %)	TEM, Zeta Potential
Shao et al. [80]	Two Step	Magnetic Stirring + Ultrasonic Agitation	239, 151, 144 nm	Deionized Water	–	–	1, (0.8 + 0.2), (0.6 + 0.4) wt. %	TEM, Zeta Potential
Khosravifard et al. [81]	Two Step	Magnetic Stirring + Ultrasonic Agitation	–	Water and Propylene (50:50)	–	Anatase	–	XRD, SEM
Jarahnejad et al. [82]	Two Step	Sonication + pH Adjustment	30 nm	Distilled Water	Polycarboxylate, Tri-oxadecane Acid	–	3–9, 9 (wt. %)	SEM, DLS
Ghadimi and Metselaar [83]	Two Step	Magnetic Stirring + Ultrasonication	Ø25 nm	Distilled Water	SDS	–	0.1 (wt. %)	TEM, UV-vis, Zeta potential
Hussein et al. [84]	Two Step	Mechanical Stirring + Ultrasonication	Ø30 nm	Distilled Water	–	–	1, 1.5, 2.0, 2.5 (vol. %)	–
Batmunkh et al. [85]	Two Step	Mechanical Stirring + Ultrasonication	15 nm, 300 nm	Distilled Water	–	–	1, 2, 3 (wt. %)	XRD, SEM
Bahiraei et al. [86]	Two Step	Magnetic Stirring + Ultrasonication	–	Water	–	–	0.1, 0.4, 0.7, 1.0 (vol. %)	–
Arani and Amani [87]	Two Step	pH adjustment + Ultrasonication	Ø (10, 20, 30, 50) nm	Distilled Water	CTAB	–	1.0, 1.5, 2.0 (vol. %)	TEM
Vakili et al. [88]	Two Step	Ultrasonication + pH Adjustment	Ø25 nm	Distilled Water, ethylene glycol/water mixture	NaOH	–	0.5, 1.0, 1.5 (vol. %)	–

References

1. Maxwell, J.C. *A Treatise on Electricity and Magnetism*; Clarendon Press: England, UK, 1873; Volume 1.
2. Masuda, H.; Ebata, A.; Teramae, K.; Hishinuma, N. Alteration of Thermal Conductivity and Viscosity of Liquid by Dispersing Ultra-Fine Particles. Dispersion of Al₂O₃, SiO₂ and TiO₂ Ultra-Fine Particles. *Netsu Bussei* **1993**, *7*, 227–233. [[CrossRef](#)]
3. Choi, S.U.S.; Eastman, J.A. Enhancing thermal conductivity of fluids with nanoparticles. *ASME Int. Mech. Eng. Congr. Expos.* **1995**, *66*, 99–105. [[CrossRef](#)]
4. Popa, I.; Gillies, G.; Papastavrou, G.; Borkovec, M. Attractive and repulsive electrostatic forces between positively charged latex particles in the presence of anionic linear polyelectrolytes. *J. Phys. Chem. B* **2010**, *114*, 3170–3177. [[CrossRef](#)] [[PubMed](#)]
5. Keblinski, P.; Phillpot, S.; Choi, S.; Eastman, J. Mechanisms of heat flow in suspension of nanosized particles (nanofluids). *Int. J. Heat Mass Transf.* **2002**, *45*, 855–863. [[CrossRef](#)]
6. Jang, S.P.; Choi, S.U.S. Role of Brownian motion in the enhanced thermal conductivity of nanofluids. *Appl. Phys. Lett.* **2004**, *84*, 4316–4318. [[CrossRef](#)]
7. Xuan, Y.; Li, Q.; Hu, W. Aggregation Structure and Thermal Conductivity of Nanofluids. *Thermodynamics* **2003**, *49*, 1038–1043. [[CrossRef](#)]
8. Rafati, M.; Hamidi, A.A.; Shariati Niasser, M. Application of nanofluids in computer cooling systems (heat transfer performance of nanofluids). *Appl. Therm. Eng.* **2012**, *45–46*, 9–14. [[CrossRef](#)]
9. Ijam, A.; Saidur, R. Nanofluid as a coolant for electronic devices (cooling of electronic devices). *Appl. Therm. Eng.* **2012**, *32*, 76–82. [[CrossRef](#)]
10. Xia, G.D.; Liu, R.; Wang, J.; Du, M. The characteristics of convective heat transfer in microchannel heat sinks using Al₂O₃ and TiO₂ nanofluids. *Int. Commun. Heat Mass Transf.* **2016**, *76*, 256–264. [[CrossRef](#)]
11. Soheli, M.R.; Saidur, R.; Sabri, M.F.M.; Kamalisarvestani, M.; Elias, M.M.; Ijam, A. Investigating the heat transfer performance and thermophysical properties of nanofluids in a circular micro-channel. *Int. Commun. Heat Mass Transf.* **2013**, *42*, 75–81. [[CrossRef](#)]
12. Khaleduzzaman, S.S.; Soheli, M.R.; Saidur, R.; Selvaraj, J. Convective performance of 0.1% volume fraction of TiO₂/water nanofluid in an electronic heat sink. *Procedia Eng.* **2015**, *105*, 412–417. [[CrossRef](#)]
13. Ali, H.M.; Arshad, W. Thermal performance investigation of staggered and inline pin fin heat sinks using water based rutile and anatase TiO₂ nanofluids. *Energy Convers. Manag.* **2015**, *106*, 793–803. [[CrossRef](#)]
14. Naphon, P.; Nakhairintr, L. Heat transfer of nanofluids in the mini-rectangular fin heat sinks. *Int. Commun. Heat Mass Transf.* **2013**, *40*, 25–31. [[CrossRef](#)]
15. Ijam, A.; Saidur, R.; Ganesan, P. Cooling of minichannel heat sink using nanofluids. *Int. Commun. Heat Mass Transf.* **2012**, *39*, 1188–1194. [[CrossRef](#)]
16. Mohammed, H.A.; Gunnasegaran, P.; Shuaib, N.H. The impact of various nanofluid types on triangular microchannels heat sink cooling performance. *Int. Commun. Heat Mass Transf.* **2011**, *38*, 767–773. [[CrossRef](#)]
17. Xuan, Y.; Duan, H.; Li, Q. Enhancement of solar energy absorption using a plasmonic nanofluid based on TiO₂/Ag composite nanoparticles. *RSC Adv.* **2014**, *4*, 16206–16213. [[CrossRef](#)]
18. Subramaniyan, A.L.; Priya, S.L.; Ilangovan, R. Energy Harvesting Through Optical Properties of TiO₂ and C-TiO₂ Nanofluid for Direct Absorption Solar Collectors. *Int. J. Renew. Energy Res.* **2015**, *5*, 542–547.
19. Kahani, M.; Heris, S.Z.; Mousavi, S.M. Experimental investigation of TiO₂/water nanofluid laminar forced convective heat transfer through helical coiled tube. *Heat Mass Transf. Stoffuebertrag.* **2014**, *50*, 1563–1573. [[CrossRef](#)]
20. Said, Z.; Sabiha, M.A.; Saidur, R.; Hepbasli, A.; Rahim, N.A.; Mekhilef, S.; Ward, T.A. Performance enhancement of a Flat Plate Solar collector using Titanium dioxide nanofluid and Polyethylene Glycol dispersant. *J. Clean. Prod.* **2015**, *92*, 343–353. [[CrossRef](#)]
21. Rashid, F.; Dawood, K.; Hashim, A.H.M.E.D. Maximizing of solar absorption by (TiO₂-water) nanofluid with glass mixture. *Int. J. Res. Eng. Technol.* **2014**, *2*, 87–90.
22. Mutuku, W.N. Ethylene glycol (EG)-based nanofluids as a coolant for automotive radiator. *Asia Pac. J. Comput. Eng.* **2016**, *3*, 1. [[CrossRef](#)]
23. Devireddy, S.; Mekala, C.S.R.; Veeredhi, V.R. Improving the cooling performance of automobile radiator with ethylene glycol water based TiO₂ nanofluids. *Int. Commun. Heat Mass Transf.* **2016**, *78*, 121–126. [[CrossRef](#)]

24. Chen, J.; Jia, J. Experimental study of TiO₂ nanofluid coolant for automobile cooling applications. *Mater. Res. Innov.* **2016**, *8917*, 1–5. [[CrossRef](#)]
25. Usri, N.A.; Azmi, W.H.; Mamat, R.; Hamid, K.A. Forced convection heat transfer using water- ethylene glycol (60:40) based nanofluids in automotive cooling system. *Int. J. Automot. Mech. Eng.* **2016**, *11*, 2747–2755. [[CrossRef](#)]
26. Hussein, A.M.; Bakar, R.A.; Kadirgama, K.; Sharma, K.V. Heat transfer enhancement using nanofluids in an automotive cooling system. *Int. Commun. Heat Mass Transf.* **2014**, *53*, 195–202. [[CrossRef](#)]
27. Yuvarajan, D.; Babu, M.D.; BeemKumar, N.; Amith Kishore, P. Experimental investigation on the influence of titanium dioxide nanofluid on emission pattern of biodiesel in a diesel engine. *Atmos. Pollut. Res.* **2018**, *9*, 47–52. [[CrossRef](#)]
28. Kumar, N.; Sonawane, S.S. Experimental study of thermal conductivity and convective heat transfer enhancement using CuO and TiO₂ nanoparticles. *Int. Commun. Heat Mass Transf.* **2016**, *76*, 98–107. [[CrossRef](#)]
29. Khedkar, R.S.; Sonawane, S.S.; Wasewar, K.L. Heat transfer study on concentric tube heat exchanger using TiO₂-water based nanofluid. *Int. Commun. Heat Mass Transf.* **2014**, *57*, 163–169. [[CrossRef](#)]
30. Tiwari, A.K.; Ghosh, P.; Sarkar, J. Performance comparison of the plate heat exchanger using different nanofluids. *Exp. Therm. Fluid Sci.* **2013**, *49*, 141–151. [[CrossRef](#)]
31. Farajollahi, B.; Etemad, S.G.; Hojjat, M. Heat transfer of nanofluids in a shell and tube heat exchanger. *Int. J. Heat Mass Transf.* **2010**, *53*, 12–17. [[CrossRef](#)]
32. Javadi, F.S.; Sadeghipour, S.; Saidur, R.; BoroumandJazi, G.; Rahmati, B.; Elias, M.M.; Sohel, M.R. The effects of nanofluid on thermophysical properties and heat transfer characteristics of a plate heat exchanger. *Int. Commun. Heat Mass Transf.* **2013**, *44*, 58–63. [[CrossRef](#)]
33. Barzegarian, R.; Moraveji, M.K.; Aloueyan, A. Experimental investigation on heat transfer characteristics and pressure drop of BPHE (brazed plate heat exchanger) using TiO₂-water nanofluid. *Exp. Therm. Fluid Sci.* **2016**, *74*, 11–18. [[CrossRef](#)]
34. Kim, H.D.; Kim, J.; Kim, M.H. Experimental studies on CHF characteristics of nano-fluids at pool boiling. *Int. J. Multiph. Flow* **2007**, *33*, 691–706. [[CrossRef](#)]
35. Trisaksri, V.; Wongwises, S. Nucleate pool boiling heat transfer of TiO₂-R141b nanofluids. *Int. J. Heat Mass Transf.* **2009**, *52*, 1582–1588. [[CrossRef](#)]
36. Ali, H.M.; Generous, M.M.; Ahmad, F.; Irfan, M. Experimental investigation of nucleate pool boiling heat transfer enhancement of TiO₂-water based nanofluids. *Appl. Therm. Eng.* **2017**, *113*, 1146–1151. [[CrossRef](#)]
37. Das, S.; Saha, B.; Bhaumik, S. Experimental study of nucleate pool boiling heat transfer of water by surface functionalization with crystalline TiO₂ nanostructure. *Appl. Therm. Eng.* **2017**, *113*, 1345–1357. [[CrossRef](#)]
38. Choi, S.U.S.; Eastman, J.A. Enhanced Heat Transfer Using Nanofluids. USA Patent 6,221,275, 24 April 2001.
39. Lee, G.J.; Kim, C.K.; Lee, M.K.; Rhee, C.K. Characterization of ethylene glycol based TiO₂ nanofluid prepared by pulsed wire evaporation (PWE) method. *Rev. Adv. Mater. Sci.* **2011**, *28*, 126–129.
40. Huang, X.; Zhang, W. Study on successively preparation of nano-TiO₂ ethanol colloids by pulsed laser ablation and fluorescence property. *Appl. Surf. Sci.* **2008**, *254*, 3403–3407. [[CrossRef](#)]
41. Liu, P.S.; Cai, W.P.; Wan, L.X.; Shi, M. Da; Luo, X.D.; Jing, W.P. Fabrication and characteristics of rutile TiO₂ nanoparticles induced by laser ablation. *Trans. Nonferr. Met. Soc. China* **2009**, *19*, s743–s747. [[CrossRef](#)]
42. Liang, C.H.; Shimizu, Y.; Sasaki, T.; Koshizaki, N. Preparation of ultrafine TiO₂ nanocrystals via pulsed-laser ablation of titanium metal in surfactant solution. *Appl. Phys. A Mater. Sci. Process.* **2005**, *80*, 819–822. [[CrossRef](#)]
43. Chang, H.; Liu, M.K. Fabrication and process analysis of anatase type TiO₂ nanofluid by an arc spray nanofluid synthesis system. *J. Cryst. Growth* **2007**, *304*, 244–252. [[CrossRef](#)]
44. Chang, H.; Lin, S.-C. Fabrication Method for a TiO₂ Nanofluid with High Roundness and Superior Dispersion Properties. *Mater. Trans.* **2007**, *48*, 836–841. [[CrossRef](#)]
45. Jwo, C.S.; Tien, D.C.; Teng, T.P.; Chang, H.; Tsung, T.T.; Liao, C.Y.; Lin, C.H. Preparation and UV characterization of TiO₂ nanoparticles synthesized by SANSS. *Rev. Adv. Mater. Sci.* **2005**, *10*, 283–288.
46. Wu, Y.; Kao, M. Using TiO₂ nanofluid additive for engine lubrication oil. *Ind. Lubr. Tribol.* **2011**, *63*, 440–445. [[CrossRef](#)]
47. Behnajady, M.A.; Eskandarloo, H.; Modirshahla, N.; Shokri, M. Investigation of the effect of sol-gel synthesis variables on structural and photocatalytic properties of TiO₂ nanoparticles. *Desalination* **2011**, *278*, 10–17. [[CrossRef](#)]

48. Sharma, A.; Karn, R.K.; Pandiyan, S.K. Synthesis of TiO₂ Nanoparticles by Sol-gel Method and Their Characterization. *J. Basic Appl. Eng. Res.* **2014**, *1*, 1–5.
49. Cesnovar, A. Preparation of nano-crystalline TiO₂ by sol-gel method using titanium tetraisopropoxide (TTIP). *Adv. Nat. Sci. Theory Appl.* **2012**, 2013–2017.
50. Vijayalakshmi, R.; Rajendran, V. Synthesis and characterization of nano-TiO₂ via different methods. *Arch. Appl. Sci. Res.* **2012**, *4*, 1183–1190. [[CrossRef](#)]
51. Zhang, Y.X.; Li, G.H.; Jin, Y.X.; Zhang, Y.; Zhang, J.; Zhang, L.D. Hydrothermal synthesis and photoluminescence of TiO₂ nanowires. *Chem. Phys. Lett.* **2002**, *365*, 300–304. [[CrossRef](#)]
52. Suzuki, Y.; Yoshikawa, S. Synthesis and thermal analyses of TiO₂-derived nanotubes prepared by the hydrothermal method. *J. Mater. Res.* **2004**, *19*, 982–985. [[CrossRef](#)]
53. Nian, J.; Teng, H. Hydrothermal Synthesis of Single-Crystalline Anatase TiO₂ Nanorods with Nanotubes as the Precursor. *J. Phys. Chem. B* **2006**, *110*, 4193–4198. [[CrossRef](#)] [[PubMed](#)]
54. Yin, H.; Wada, Y.; Kitamura, T.; Kambe, S.; Murasawa, S.; Mori, H.; Sakata, T.; Yanagida, S. Hydrothermal synthesis of nanosized anatase and rutile TiO₂ using amorphous phase TiO₂. *J. Mater. Chem.* **2001**, *11*, 1694–1703. [[CrossRef](#)]
55. Pavasupree, S.; Jitputti, J.; Ngamsinlapasathian, S.; Yoshikawa, S. Hydrothermal synthesis, characterization, photocatalytic activity and dye-sensitized solar cell performance of mesoporous anatase TiO₂ nanopowders. *Mater. Res. Bull.* **2008**, *43*, 149–157. [[CrossRef](#)]
56. Corradi, A.B.; Bondioli, F.; Focher, B.; Ferrari, A.M.; Grippo, C.; Mariani, E.; Villa, C. Conventional and microwave-hydrothermal synthesis of TiO₂ nanopowders. *J. Am. Ceram. Soc.* **2005**, *88*, 2639–2641. [[CrossRef](#)]
57. Leena, M.; Srinivasan, S. Synthesis and ultrasonic investigations of titanium oxide nanofluids. *J. Mol. Liq.* **2015**, *206*, 103–109. [[CrossRef](#)]
58. Tajik, B.; Abbassi, A.; Saffar-Avval, M.; Najafabadi, M.A. Ultrasonic properties of suspensions of TiO₂ and Al₂O₃ nanoparticles in water. *Powder Technol.* **2012**, *217*, 171–176. [[CrossRef](#)]
59. Mo, S.; Chen, Y.; Jia, L.; Luo, X. Investigation on crystallization of TiO₂-water nanofluids and deionized water. *Appl. Energy* **2012**, *93*, 65–70. [[CrossRef](#)]
60. Murshed, S.M.S.; Leong, K.C.; Yang, C. Enhanced thermal conductivity of TiO₂-Water based nanofluids. *Int. J. Therm. Sci.* **2005**, *44*, 367–373. [[CrossRef](#)]
61. Palabiyik, I.; Musina, Z.; Witharana, S.; Ding, Y. Dispersion stability and thermal conductivity of propylene glycol-based nanofluids. *J. Nanopart. Res.* **2011**, *13*, 5049–5055. [[CrossRef](#)]
62. Tavman, I.; Turgut, A.; Chirtoc, M.; Hadjov, K.; Fudym, O.; Tavman, S. Experimental study on thermal conductivity and viscosity of water-based nanofluids. *Heat Transf. Res.* **2010**, *41*. [[CrossRef](#)]
63. Shu, R.; Gan, Y.; Lv, H.; Tan, D. Preparation and rheological behavior of ethylene glycol-based TiO₂ nanofluids. *Colloids Surfaces A Physicochem. Eng. Asp.* **2016**, *509*, 86–90. [[CrossRef](#)]
64. Birlik, I.; Azem, N.F.A.; Yiğit, R.; Erol, M.; Yildirim, S.; Sancakoğlu, O.; Çelik, E. Preparation and Characterization of TiO₂ Nanofluid by Sol-gel Method for Cutting Tools Kesici Takımlar İçin Sol-jel Metoduyla TiO₂ Nano sıvıların Hazırlanması ve Karakterizasyonu. *Afyon Kocatepe Üniversitesi Fen ve Mühendislik Bilimleri Dergisi* **2014**, *14*, 453–460.
65. Duangthongsuk, W.; Wongwises, S. Heat transfer enhancement and pressure drop characteristics of TiO₂-water nanofluid in a double-tube counter flow heat exchanger. *Int. J. Heat Mass Transf.* **2009**, *52*, 2059–2067. [[CrossRef](#)]
66. Yiamsawas, T.; Dalkilic, A.S.; Mahian, O.; Wongwises, S. Measurement and Correlation of the Viscosity of Water-Based Al₂O₃ and TiO₂ Nanofluids in High Temperatures and Comparisons with Literature Reports. *J. Dispers. Sci. Technol.* **2013**, *34*, 1697–1703. [[CrossRef](#)]
67. Turgut, A.; Tavman, I.; Chirtoc, M.; Schuchmann, H.P.; Sauter, C.; Tavman, S. Thermal Conductivity and Viscosity Measurements of Water-Based TiO₂ Nanofluids. *Int. J. Thermophys.* **2009**, *30*, 1213–1226. [[CrossRef](#)]
68. Kayhani, M.H.; Soltanzadeh, H.; Heyhat, M.M.; Nazari, M.; Kowsary, F. Experimental study of convective heat transfer and pressure drop of TiO₂/water nanofluid. *Int. Commun. Heat Mass Transf.* **2012**, *39*, 456–462. [[CrossRef](#)]
69. Yoo, D.H.; Hong, K.S.; Yang, H.S. Study of thermal conductivity of nanofluids for the application of heat transfer fluids. *Thermochim. Acta* **2007**, *455*, 66–69. [[CrossRef](#)]
70. Kim, S.H.; Choi, S.R.; Kim, D. Thermal Conductivity of Metal-Oxide Nanofluids: Particle Size Dependence and Effect of Laser Irradiation. *J. Heat Transf.* **2007**, *129*, 298. [[CrossRef](#)]

71. Saleh, R.; Putra, N.; Wibowo, R.E.; Septiadi, W.N.; Prakoso, S.P. Titanium dioxide nanofluids for heat transfer applications. *Exp. Therm. Fluid Sci.* **2014**, *52*, 19–29. [[CrossRef](#)]
72. Chakraborty, S.; Sarkar, I.; Behera, D.K.; Pal, S.K.; Chakraborty, S. Experimental investigation on the effect of dispersant addition on thermal and rheological characteristics of TiO₂ nanofluid. *Powder Technol.* **2017**, *307*, 10–24. [[CrossRef](#)]
73. Kavitha, T.; Rajendran, A.; Durairajan, A. Synthesis, characterization of TiO₂ nano powder and water based nanofluids using two step method. *Eur. J. Appl. Eng. Sci. Res.* **2012**, *1*, 235–240.
74. Mansour, D.E.A.; Atiya, E.G.; Khattab, R.M.; Azmy, A.M. Effect of Titania Nanoparticles on the Dielectric Properties of Transformer Oil-Based Nanofluids. In Proceedings of the 2012 Annual Report Conference on Electrical Insulation and Dielectric Phenomena (CEIDP), Montreal, QC, Canada, 14–17 October; pp. 295–298.
75. Elsalamony, R.A.; Morsi, R.E.; Alsabagh, A.M. *Preparation, Stability and Photocatalytic Activity of Titania Nanofluid Using Gamma Irradiated Titania Nanoparticles by Two-Step Method*; Radwa, A., Elsalamony, R.E., Morsi, A.M., Eds.; Alsabagh Egyptian Petroleum Research Institute (EPRI): Cairo, Egypt, 2015; pp. 1–13.
76. Li, S.; Sun, W. A comparative study on aggregation/sedimentation of TiO₂nanoparticles in mono- and binary systems of fulvic acids and Fe(III). *J. Hazard. Mater.* **2011**, *197*, 70–79. [[CrossRef](#)] [[PubMed](#)]
77. He, Y.; Jin, Y.; Chen, H.; Ding, Y.; Cang, D.; Lu, H. Heat transfer and flow behaviour of aqueous suspensions of TiO₂ nanoparticles (nanofluids) flowing upward through a vertical pipe. *Int. J. Heat Mass Transf.* **2007**, *50*, 2272–2281. [[CrossRef](#)]
78. Wen, D.; Ding, Y. Formulation of nanofluids for natural convective heat transfer applications. *Int. J. Heat Fluid Flow* **2005**, *26*, 855–864. [[CrossRef](#)]
79. Wei, B.; Zou, C.; Li, X. Experimental investigation on stability and thermal conductivity of diathermic oil based TiO₂ nanofluids. *Int. J. Heat Mass Transf.* **2017**, *104*, 537–543. [[CrossRef](#)]
80. Shao, X.; Chen, Y.; Mo, S.; Cheng, Z.; Yin, T. Dispersion Stability of TiO₂-H₂O Nanofluids Containing Mixed Nanotubes and Nanosheets. *Energy Procedia* **2015**, *75*, 2049–2054. [[CrossRef](#)]
81. Khosravifard, E.; Salavati-Niasari, M. Synthesis and Characterization of TiO₂-CNTs Nanocomposite and Investigation of Viscosity and Thermal Conductivity of a New Nanofluid. *J. Nanostruct.* **2012**, *2*, 191–197.
82. Jarahnejad, M.; Haghghi, E.B.; Saleemi, M.; Nikkam, N.; Khodabandeh, R.; Palm, B.; Toprak, M.S.; Muhammed, M. Experimental investigation on viscosity of water-based Al₂O₃ and TiO₂ nanofluids. *Rheol. Acta* **2015**, *54*, 411–422. [[CrossRef](#)]
83. Ghadimi, A.; Metselaar, I.H. The influence of surfactant and ultrasonic processing on improvement of stability, thermal conductivity and viscosity of titania nanofluid. *Exp. Therm. Fluid Sci.* **2013**, *51*, 1–9. [[CrossRef](#)]
84. Adnan, M.; Hussein, R.A.; Bakar, K.K.; Sharma, K.V. Experimental Measurement of. *Energy* **2013**, *7*, 850–863.
85. Batmunkh, M.; Myekhlai, M.; Choi, H.; Chung, H.; Jeong, H. Thermal Conductivity of TiO₂ Nanoparticles Based Aqueous Nano fluids with an Addition of a Modified Silver Particle. *Ind. Eng. Chem. Res.* **2014**, *53*, 8445–8451. [[CrossRef](#)]
86. Bahiraei, M.; Hosseinalipour, S.M.; Zabihi, K.; Taheran, E. Using Neural Network for Determination of Viscosity in Water-TiO₂ Nanofluid. *Adv. Mech. Eng.* **2012**, *4*, 1–10. [[CrossRef](#)]
87. Arani, A.A.; Amani, J. Experimental investigation of diameter effect on heat transfer performance and pressure drop of TiO₂-water nanofluid. *Exp. Therm. Fluid Sci.* **2013**, *44*, 520–533. [[CrossRef](#)]
88. Vakili, M.; Mohebbi, A.; Hashemipour, H. Experimental study on convective heat transfer of TiO₂ nanofluids. *Heat Mass Transf. Stoffuebertrag.* **2013**, *49*, 1159–1165. [[CrossRef](#)]
89. Hamilton, R.L.; Crosser, O. Thermal conductivity of heterogeneous two-component systems. *Ind. Eng. Chem. Fundam.* **1962**, *1*, 187–191. [[CrossRef](#)]
90. Nan, C.W.; Birringer, R.; Clarke, D.R.; Gleiter, H. Effective thermal conductivity of particulate composites with interfacial thermal resistance. *J. Appl. Phys.* **1997**, *81*, 6692–6699. [[CrossRef](#)]
91. Bruggeman, D.A.G. Berechnung verschiedener physikalischer Konstanten von heterogenen Substanzen. III. Die elastischen Konstanten der quasiisotropen Mischkörper aus isotropen Substanzen. *Ann. Phys.* **1937**, *421*, 160–178. [[CrossRef](#)]
92. Wasp, F.J.; Kenny, J.P.; Gandhi, R.L. *Solid-Liquid Slurry Pipeline Transportation*; Trans Tech Publication: Clausthal, Germany, 1977.

93. Xie, H.; Fujii, M.; Zhang, X. Effect of interfacial nanolayer on the effective thermal conductivity of nanoparticle-fluid mixture. *Int. J. Heat Mass Transf.* **2005**, *48*, 2926–2932. [[CrossRef](#)]
94. Yu, W.; Choi, S.U.S. The role of interfacial layers in the enhanced thermal conductivity of nanofluids: A renovated Maxwell model. *J. Nanopart. Res.* **2003**, *5*, 167–171. [[CrossRef](#)]
95. Wang, W.; Lin, L.; Zhou, X.; Wang, S. A Comprehensive Model for the Enhanced Thermal Conductivity of Nanofluids. *J. Adv. Res. Phys.* **2012**, *3*, 1–5.
96. Chandrasekar, M.; Suresh, S.; Srinivasan, R.; Bose, A.C. New Analytical Models to Investigate Thermal Conductivity of Nanofluids. *J. Nanosci. Nanotechnol.* **2009**, *9*, 533–538. [[CrossRef](#)] [[PubMed](#)]
97. Avsec, J.; Oblak, M. The calculation of thermal conductivity, viscosity and thermodynamic properties for nanofluids on the basis of statistical nanomechanics. *Int. J. Heat Mass Transf.* **2007**, *50*, 4331–4341. [[CrossRef](#)]
98. Corcione, M. Empirical correlating equations for predicting the effective thermal conductivity and dynamic viscosity of nanofluids. *Energy Convers. Manag.* **2011**, *52*, 789–793. [[CrossRef](#)]
99. Fedele, L.; Colla, L.; Bobbo, S. Viscosity and thermal conductivity measurements of water-based nanofluids containing titanium oxide nanoparticles. *Int. J. Refrig.* **2012**, *35*, 1359–1366. [[CrossRef](#)]
100. Hamid, K.A.; Azmi, W.H.; Mamat, R.; Usri, N.A.; Najafi, G. Effect of temperature on heat transfer coefficient of titanium dioxide in ethylene glycol-based nanofluid. *J. Mech. Eng. Sci.* **2015**, *8*, 1367–1375. [[CrossRef](#)]
101. Duangthongsuk, W.; Wongwises, S. Measurement of temperature-dependent thermal conductivity and viscosity of TiO₂-water nanofluids. *Exp. Therm. Fluid Sci.* **2009**, *33*, 706–714. [[CrossRef](#)]
102. Hojjat, M.; Etemad, S.G.; Bagheri, R.; Thibault, J. Thermal conductivity of non-Newtonian nanofluids: Experimental data and modeling using neural network. *Int. J. Heat Mass Transf.* **2011**, *54*, 1017–1023. [[CrossRef](#)]
103. Hu, Y.; He, Y.; Wang, S.; Wang, Q.; Inaki Schlager, H. Experimental and Numerical Investigation on Natural Convection Heat Transfer of TiO₂-Water Nanofluids in a Square Enclosure. *J. Heat Transfer* **2013**, *136*, 22502. [[CrossRef](#)]
104. Islam, M.R.; Shabani, B.; Rosengarten, G. Electrical and Thermal Conductivities of 50/50 Water-ethylene Glycol Based TiO₂ Nanofluids to be Used as Coolants in PEM Fuel Cells. *Energy Procedia* **2017**, *110*, 101–108. [[CrossRef](#)]
105. Pak, B.C.; Cho, Y.I. Hydrodynamic and heat transfer study of dispersed fluids with submicron metallic oxide particles. *Exp. Heat Transf. Int. J.* **2007**, 37–41. [[CrossRef](#)]
106. Esfe, M.H.; Nadooshan, A.A.; Arshi, A.; Alirezaie, A. Convective heat transfer and pressure drop of aqua based TiO₂ nanofluids at different diameters of nanoparticles: Data analysis and modeling with artificial neural network. *Phys. E Low-Dimension. Syst. Nanostruct.* **2018**, *97*, 155–161. [[CrossRef](#)]
107. Fan, X.; Chen, H.; Ding, Y.; Plucinski, P.K.; Lapkin, A.A. Potential of “nanofluids” to further intensify microreactors. *Green Chem.* **2008**, *10*, 670. [[CrossRef](#)]
108. Einstein, A. Eine neue Bestimmung der Moleküldimensionen. *Ann. Phys.* **1906**, *324*, 289–306. [[CrossRef](#)]
109. Brinkman, H.C. The Viscosity of Concentrated Suspensions and Solutions. *J. Chem. Phys.* **1952**, *20*, 571. [[CrossRef](#)]
110. Batchelor, G.K. Effect of Brownian-motion on bulk stress in a suspension of spherical-particles. *J. Fluid Mech.* **1977**, *83*, 97–117. [[CrossRef](#)]
111. Nielsen, L.E. Generalized equation for the elastic moduli of composite materials. *J. Appl. Phys.* **1970**, *41*, 4626–4627. [[CrossRef](#)]
112. Bobbo, S.; Fedele, L.; Benetti, A.; Colla, L.; Fabrizio, M.; Pagura, C.; Barison, S. Viscosity of water based swcnh and TiO₂ nanofluids. *Exp. Therm. Fluid Sci.* **2012**, *36*, 65–71. [[CrossRef](#)]
113. Chen, H.; Ding, Y.; Tan, C. Rheological behaviour of nanofluids. *New J. Phys.* **2007**, *9*. [[CrossRef](#)]
114. Chen, H.; Ding, Y.; He, Y.; Tan, C. Rheological behaviour of ethylene glycol based titania nanofluids. *Chem. Phys. Lett.* **2007**, *444*, 333–337. [[CrossRef](#)]
115. Tseng, W.J.; Lin, K.C. Rheology and colloidal structure of aqueous TiO₂ nanoparticle suspensions. *Mater. Sci. Eng. A* **2003**, *355*, 186–192. [[CrossRef](#)]
116. Chevalier, J.; Tillement, O.; Ayela, F. Structure and rheology of SiO₂ nanoparticle suspensions under very high shear rates. *Phys. Rev.* **2009**, *80*, 1–7. [[CrossRef](#)]

117. Teng, T.P.; Hung, Y.H.; Jwo, C.S.; Chen, C.C.; Jeng, L.Y. Pressure drop of TiO₂ nanofluid in circular pipes. *Particuology* **2011**, *9*, 486–491. [[CrossRef](#)]
118. Sen, S.; Govindarajan, V.; Pelliccione, C.J.; Wang, J.; Miller, D.J.; Timofeeva, E.V. Surface Modification Approach to TiO₂ Nanofluids with High Particle Concentration, Low Viscosity, and Electrochemical Activity. *ACS Appl. Mater. Interfaces* **2015**, *7*, 20538–20547. [[CrossRef](#)] [[PubMed](#)]



© 2018 by the authors. Licensee MDPI, Basel, Switzerland. This article is an open access article distributed under the terms and conditions of the Creative Commons Attribution (CC BY) license (<http://creativecommons.org/licenses/by/4.0/>).